Title	Stimulation of nuclear receptor REV-ERBs suppresses production of pronociceptive molecules in cultured spinal astrocytes and ameliorates mechanical hypersensitivity of inflammatory and neuropathic pain of mice
Author(s)	Morioka, Norimitsu; Kodama, Keitaro; Tomori, Mizuki; Yoshikawa, Kanade; Saeki, Munenori; Nakamura, Yoki; Zhang, Fang Fang; Hisaoka-Nakashima, Kazue; Nakata, Yoshihiro
Citation	Brain, Behavior, and Immunity , 78 : 116 - 130
Issue Date	2019-05
DOI	10.1016/j.bbi.2019.01.014
Self DOI	
URL	https://ir.lib.hiroshima-u.ac.jp/00048640
Right	© 2019. This manuscript version is made available under the CC-BY-NC-ND 4.0 license http://creativecommons.org/licenses/by-nc-nd/4.0/ This is not the published version. Please cite only the published version. この論文は出版社版でありません。引用の際には出版社版をご確認、ご利用ください。
Relation	

Stimulation of nuclear receptor REV-ERBs suppresses production of pronociceptive molecules in cultured spinal astrocytes and ameliorates mechanical hypersensitivity of inflammatory and neuropathic pain of mice

Norimitsu Morioka[1)], Keitaro Kodama[1)], Mizuki Tomori[1)], Kanade Yoshikawa[1)], Munenori Saeki[1)], Yoki Nakamura[1), 2)], Fang Fang Zhang[1), 3)], Kazue Hisaoka-Nakashima[1)], Yoshihiro Nakata[1)]

1) Department of Pharmacology, Hiroshima University Graduate School of Biomedical & Health Sciences, 1-2-3 Kasumi, Minami-ku, Hiroshima 734-8553, Japan

2) Cellular Pathobiology Section, Integrative Neuroscience Research Branch, National Institute on Drug Abuse IRP, Triad Suite 3305, 333 Cassell Drive, Baltimore, MD 21224

3) Institute of Pharmacology, Taishan Medical University, 619 Changcheng Road, Taian, Shandong 271016, China

Corresponding author; Norimitsu MORIOKA
Address: Kasumi 1-2-3, Minami-ku, Hiroshima 734-8553, Japan
Tel: +81-82-257-5312, Fax: +81-82-257-5314,
e-mail: mnori@hiroshima-u.ac.jp

Number of pages: 46, Number of figures: 10, Number of words: 8505

The authors declare no competing financial interests.

Abstract

The orphan nuclear receptors REV-ERBα and REV-ERBβ (REV-ERBs) are crucial in the regulation of inflammatory-related gene transcription in astroglioma cells, but their role in nociceptive transduction has yet to be elaborated. Spinal dorsal horn astrocytes contribute to the maintenance of chronic pain. Treatment of cultured spinal astrocytes with specific REV-ERBs agonists SR9009 or GSK4112 significantly prevented lipopolysaccharide (LPS)-induced mRNA upregulation of pronociceptive molecules interleukin-1β (IL-1β) mRNA, interleukin-6 (IL-6) mRNA and matrix metalloprotease-9 (MMP-9) mRNA, but not CCL2 mRNA expression. Treatment with SR9009 also blocked tumor necrosis factor-induced IL-1β mRNA, IL-6 mRNA and MMP-9 mRNA. In addition, treatment with SR9009 significantly blocked LPS-induced upregulation of IL-1β protein, IL-6 protein and MMP-9 activity. The inhibitory effects of SR9009 on LPS-induced expression of pronociceptive molecules were blocked by knockdown of REV-ERBs expression with short interference RNA, confirming that SR9009 exerts its effect through REV-ERBs. Intrathecal LPS treatment in male mice induces hind paw mechanical hypersensitivity, and upregulation of IL-1β mRNA, IL-6 mRNA and glial fibrillary acidic protein (GFAP) expression in spinal dorsal horn. Intrathecal pretreatment of SR9009 prevented the onset of LPS-induced mechanical hypersensitivity, cytokine expression and GFAP expression. Intrathecal injection of

SR9009 also ameliorated mechanical hypersensitivity during the maintenance phase of complete Freund's adjuvant-induced inflammatory pain and partial sciatic nerve ligation-, paclitaxel-, and streptozotocin-induced neuropathy in mice. The current findings suggest that spinal astrocytic REV-ERBs could be critical in the regulation of nociceptive transduction through downregulation of pronociceptive molecule expression. Thus, spinal REV-ERBs could be an effective therapeutic target in the treatment of chronic pain.

Keywords

REV-ERBs; chronic pain; astrocyte; spinal dorsal horn; interleukin-1β; interleukin-6; tumor necrosis factor; siRNA

Abbreviations

CFA; complete Freund's adjuvant, DMEM; Dulbecco's modified Eagle's medium, FCS; fetal calf serum, GAPDH; glyceraldehydes-3-phosphate dehydrogenase, HDAC; histone deacetylase, iNOS; inducible nitric oxide synthase, IL-1β; interleukin-1β, IL-6; interleukin-6, LPS; lipopolysaccharide, MMP; matrix metalloproteinase, NF-κB; nuclear factor-κB, PBS; phosphate buffered saline, PSNL; partial sciatic nerve ligation, siRNA; small interference RNA , TNF; tumor necrosis factor,

Introduction

There are an increasing number patients suffering from chronic pain, including neuropathic and inflammatory pain, which is associated with the growing population of elderly people (Ferreira and de Luca, 2017; Gagliese et al., 2017). In addition, for many of these patients, chronic pain is refractory to treatment with commonly used analgesics such as opioids and non-steroidal anti-inflammatory drugs. A number of studies have shown that dysregulation of the expression of a number of pronociceptive factors such as pro-inflammatory cytokines and chemokines in CNS glial cells contribute to the induction and maintenance of chronic pain (Grace et al., 2014; Ji et al., 2016). While antagonists, neutralizing antibodies and synthesis blockers to pronociceptive molecules show varying degrees of efficacy in a range of chronic pain models, the analgesic effects of these reagents alone are not always robust. This suggests that targeting mechanisms that regulate the production of numerous molecules rather than targeting specific molecules may be crucial in alleviating chronic pain.

REV-ERBα and REV-ERBβ (REV-ERBs) are orphan nuclear receptors encoded by NR1D1 and NR1D2, respectively, which are expressed in various cell types (Kojetin and Burris, 2014). It has been demonstrated that REV-ERBs have crucial functions in the regulation of metabolism, inflammation and tumor growth (Sato et al., 2014; Solt et

al., 2012; Sulli et al., 2018). Like other nuclear receptors, REV-ERBs exert a ligand-dependent inhibitory effect on gene transcription of various molecules (Kojetin and Burris, 2014; Yin and Lazar, 2005). Accumulating evidence has shown that REV-ERBs negatively regulate the expression of various proinflammatory molecules such as the cytokine interleukin-6 (IL-6) and the chemokine CCL2, following binding of the synthetic REV-ERB-specific agonists GSK4112 and SR9009 in macrophages (Sato et al., 2014; Sitaula et al., 2015). A previous finding showed mildly increased mechanical nociceptive sensitivity in REV-ERBα knockout mice (Lee et al., 2016). Furthermore, it is possible that REV-ERBs might be a new target as analgesic for osteoarthritis-induced pain (Das et al., 2018). However, the exact function and role of REV-ERBs in nociceptive transduction under chronic pain states has yet to be elaborated.

Over-activation of astrocytes in spinal dorsal horn contributes to the maintenance of chronic pain (Morioka et al., 2015; Zhuang et al., 2005). Production of pronociceptive molecules by spinal astrocytes could lead to persistent nociceptive hypersensitivity (Gao et al., 2009; Mika et al., 2013; Nakagawa and Kaneko, 2010). Intrathecal administration of fluorocitrate, an astrocytic inhibitor, ameliorated nociceptive hypersensitivity in chronic pain models (Shibata et al., 2011; Zhang et al., 2012b). These observations suggest that modulating spinal astrocytic activity, from an abnormal or pathophysiological state back to the normal, physiological state, could be

crucial in reducing or eliminating nociceptive hypersensitivity.

Stimulation of REV-ERBs expressed in C6 astroglioma cells suppressed cytokine tumor necrosis factor (TNF)-induced expression of both CCL2 and matrix metalloprotease-9 (MMP-9) (Morioka et al., 2016b). However, a role for REV-ERBs in regulating spinal astrocytic function and in nociceptive transduction in particular has yet to be elaborated. Thus, the current study examined the effects of synthetic REV-ERBs specific agonists SR9009 and GSK4112 on REV-ERBs expressed on spinal astrocytes. The endotoxin lipopolysaccharide (LPS) elicits robust neuroinflammation in animal models and is widely used to induce inflammatory pain through activation of astrocytes in the CNS (Li et al., 2014; Lu et al., 2015). The current study examined the effect of REV-ERBs specific agonists on LPS-induced expression of pro-nociceptive molecules by spinal astrocytes and the antinociceptive effects of SR9009 on LPS-induced mechanical hypersensitivity and inflammatory and neuropathic pain in mice.

Materials and Methods

Animals

All experiments utilizing animals were conducted in accordance with the “Guidelines for the Care and Use of Laboratory Animals” established by The Japanese Pharmacological Society and Hiroshima University, and procedures were reviewed and approved by the Committee of Research Facilities for Laboratory Animal Science of Hiroshima University.

Pregnant Wistar rats (13 days) were obtained from Japan SLC, Inc. (Shizuoka, Japan) and 1-day old pups of both sexes were obtained from these rats. Male ddy mice, 6 weeks of age (Japan SLC, Inc.) were maintained in a vivarium, room temperature of 22±2℃, with a 12h light/dark cycle (lights on/off at 8:00 AM/8:00 PM), and given access to food and water available *ad libitum* during the experimental period.

Reagents

Lipopolysaccharide was obtained from Sigma Chemical Co. (St. Louis, MO, USA). SR9009, a REV-ERBs agonist (REV-ERBα EC_{50}=0.67 μM, REV-ERBβ EC_{50}=0.8 μM (Solt et al., 2012)), was obtained from Merck Millipore (Darmastadt, Germany). GSK4112 was purchased from Cayman Chemical (Ann Arbor, MI). GSK4112 is a

synthetic REV-ERBs agonist (The 50% effective concentration (EC_{50}) to REV-ERBα is 0.4 μM. The EC_{50} to REV-ERBβ is not known.) (Grant et al., 2010). RGFP966 is a selective histone deacetylase 3 (HDAC3) inhibitor (50% inhibitory concentration (IC_{50})=0.08 μM), and is reported to have no affinity to other types of HDAC (IC_{50}>15 μM). GSK4112, SR9009 and RGFP966 were dissolved in DMSO to a final concentration of 0.1% DMSO. Recombinant rat TNF was obtained from WAKO Pure Chemical Industries (Osaka, Japan). TNF was dissolved in distilled H_2O. Paclitaxel was obtained from Sawai Pharmaceutical Co., Ltd. (Osaka, Japan).

Cell culture

The preparation of cultured spinal astrocytes has been described previously (Morioka et al., 2018). In brief, spinal cords isolated from neonatal Wistar rats were minced, and then incubated with trypsin and DNase Ⅰ. Dissociated cells were suspended in Dulbecco's modified Eagle's medium (DMEM) supplemented with 10% fetal calf serum (FCS) and penicillin/streptomycin (100 units/ml and 100 μg/ml, respectively). Thereafter, cell suspensions were plated in 75cm^2 tissue culture flasks (7.5-10×10^6 cells/flask) precoated with poly-L-lysine (10 μg/ml). Cells were maintained in a 10% CO_2 incubator at 37℃. After 10 days, the flasks containing mixed glial cells were vigorously shaken and washed with PBS to remove microglial cells.

Remaining cells were trypsinized, and seeded to new flasks. After confluent state, cells were treated with 1 μM of cytosine β-D-arabinofuranoside (Sigma) to prevent proliferation of other cells such as microglia and fibroblasts for 2 days. Then, the flasks were again vigorously shaken and washed, and the cells were trypsinized. Thereafter, the remaining cells were transferred to 35-mm dishes (3-3.5×10^5 cells). After 3 days, the medium was replaced with DMEM without FCS and antibiotics. After an additional 24 hours of incubation, the cells were used in experiments. Greater than 95% of the cells obtained using the current method expressed an astrocytic phenotype as confirmed by RT-PCR and Western blotting (Morioka et al., 2014).

Rat cultured spinal astrocytes have been shown to express Rev-erbα mRNA and Rev-erbβ mRNA (Morioka et al., 2016b). To induce expression of pro-nociceptive molecules, cells were incubated with either LPS (10 ng/ml) or TNF (10 ng/ml). The role of REV-ERBs in LPS-induced gene expression was assessed using pharmacological agents. Compounds that activated REV-ERB were incubated in astrocytes for 30 min followed by LPS or TNF incubation for up to 24 hours. Cell medium and cells were removed for assay at specific time points during LPS or TNF incubation (see Results).

Real-time PCR analysis

cDNA synthesized using 1 μg of total RNA from cultured spinal astrocytes and mice spinal tissue were subjected to real-time PCR assay with specific primers and EXPRESS SYBR® GreenER™ qPCR SuperMix (Invitrogen, Carlsbad, CA, USA). The sequences of the primers are described in previous reports (Morioka et al., 2018; Zhang et al., 2016). Real-time PCR assays were conducted using a DNA engine Opticon 2 real-time PCR detection system (Bio-Rad, Hercules, CA, USA). The three-step amplification protocol consisted of 3 min at 95℃ followed by 40 cycles of 95℃ for 15 s, 60℃ for 30 s, and 72℃ for 30 s. RNA quantification of target genes was calculated using the C_t method. The C_t values of each amplification were normalized to those obtained with the amplification of glyceraldehydes-3-phosphate dehydrogenase (GAPDH).

Transfection of primary cultured astrocytes with small interfering RNA (siRNA)

Forty-eight hours after the cells were seeded, the culture was replaced with Opti-MEM medium (Invitrogen, Carlsbad, CA, USA), and then the cells were transfected with either siRNA, targeting rat *Rev-erbα* (siGENOME SMARTpool, Rat Nr1d1, GE Dharmacon, Lafayette, CO, USA), *Rev-erbβ* (siGENOME SMARTpool, Rat Nr1d2, GE Dharmacon) or non-targeting siRNA (siGENOME Non-Targeting siRNA Pool #2) by using Lipofectamine RNAi MAX reagent (Invitrogen). Twenty-four hours after

transfection, cells were treated with SR9009 for 30 min. Then, cells were further treated with LPS for 24 hours.

ELISA

Rat IL-1β, IL-6 and CCL2 protein levels in cell-conditioned medium were measured using ELISA kits (eBioscience, San Diego, CA, USA). After treatment with SR9009 for 30 min, astrocytes were stimulated with LPS for 24 hours. Then, culture media were immediately collected and stored at -80℃ until assay. Each reaction was performed according to the manufacturer's protocol.

Gelatin zymography

To measure the activity of MMP-9, a gelatinase, gelatin zymography was performed based on methods described previously (Abe et al., 2016). In brief, after drug treatment, the culture supernatant of primary astrocytes was collected, and the supernatant was added to sample buffer (125 mM Tris-HCl, pH 6.8, 1% glycerol, 2% SDS, 0.01% bromophenol blue), and equal amount of protein were separated by electrophoresis using 8% SDS-polyacrylamide gel containing 0.1% gelatin under non-reducing condition. After separation, gels were incubated with 2.5% Triton X-100 for 1 hour, and further incubated with the buffer (50 mM Tris-HCl (pH 7.4, 10 mM $CaCl_2$,

0.02% NaN_3) for 20 hours at 37℃. Then, gels were incubated with the staining solution (0.125% Coomassie Brilliant Blue R-250, 30% ethanol, 10% acetic acid) for 3 hours, and destained in 25% methanol/7.5% acetic acid until bands showing gelatinolysis are clearly appeared. The density of specific band for MMP-9 was identified dependent on the molecular size (83 kDa) of MMP-9 described previous study (Abe et al., 2016) and using by the MMP Marker (PMC Cosmobio, Tokyo, Japan). The density was measured with Science Lab Image Gauge (Fuji Film, Tokyo, Japan).

Mouse intrathecal injection

Intrathecal injections were performed on unanesthetized mice. In brief, mice were restrained with the left hand and the injection was performed with the right hand. The vertebral landmarks for L5 and L6 vertebrate were identified by palpation. An injection into the subarachnoid space between the L5 and the L6 vertebrae was done via a 27-gage needle. Entry of the needle was confirmed with the presence of a tail flick. The injection volume of all other compounds was 5 μl.

Inflammatory pain models

Inflammation was induced by either intrathecal injection of LPS (0.1 μg/5 μl saline) or

subcutaneous injection of complete Freund's adjuvant (CFA; 30 μl, 1mg of Mycobacterium tuberculosis/ml, Sigma) into the center of the plantar surface of left hind-paw in mice. The same volume of saline was used as a control.

Partial sciatic nerve ligation (PSNL)-induced neuropathic pain model

Under sodium pentobarbital (50 mg/kg, i.p.) anesthesia, a tight ligation of approximately one-third to one-half of the diameter of the left sciatic nerve (ipsilateral) was performed with 8-0 silk suture as described previously (Morioka et al., 2016a). In sham-operated mice, the sciatic nerve was exposed but not ligation. Previous studies have demonstrated that mechanical hypersensitivity was observed 3 days, and lasted at 3 weeks following PSNL (Morioka et al., 2015; Nakamura et al., 2015).

Paclitaxel-induced neuropathic pain model

Paclitaxel was dissolved in cremophor:ethanol (1:1) as the stock solution (6 mg/ml). This was diluted in saline to a final concentration of 0.2 mg/ml. The vehicle for paclitaxel was diluted with saline at the same proportion as the paclitaxel solution. Then, paclitaxel (2 mg/kg) was intraperitoneally administered in a volume of 0.1 mL/20 g once per day for 5 times every other day (cumulative dose 10 mg/kg).

Diabetes-induced neuropathic pain model

Diabetes was induced in mice fasted overnight by an injection of streptozotocin (Cayman Chemical). Streptozotocin was dissolved in saline immediately before injection and the solution administered intraperitoneally at a dose of 200 mg/kg. Control animals received a vehicle injection. Blood samples were collected from tail vein, and blood glucose levels were measured by a glucometer (Freestyle Freedom Lite; NIPRO, Osaka, Japan). Hyperglycemic mice (>300 mg/dl) at 21 days after streptozotocin injection were used for further analysis.

Hind paw sensitivity to mechanical stimulation

All behavioral assessments were performed blinded. The withdrawal threshold (in grams) of the hind paw to mechanical stimulation was determined using von Frey filaments (Morioka et al., 2015). In brief, a von Frey filament was pressed against the mid-planter surface of the hind paw. The lowest force that caused responses such as lifting and licking of the hind paw was assigned as the withdrawal threshold. Each hind paw was tested three times, at 10 second intervals, and the mean withdrawal threshold was reported. Mice with inflammation, PSNL or paclitaxel that did not show robust mechanical hypersensitivity, hind paw withdrawal threshold >0.1 g, were excluded from the experiments. Prior to treatment, hind paw withdrawal thresholds

were 1.0±0.2 g (mean±SEM).

In LPS-treated mice, either 100 or 300 nmol of SR9009 or 100 nmol of GSK4112 were intrathecally treated 1 hour before LPS injection. Withdrawal thresholds were measured 1, 2, 3, 6 and 24 hours following the second intrathecal injection. In CFA-treated mice, 7 days following intraplantar treatment of CFA, mice received either an intrathecal treatment of 100 or 300 nmol of SR9009 or 100 nmol of GSK4112. Withdrawal thresholds were then measured 1, 2, 3, 6 and 24 hours post-injection. In PSNL mice, 14 days following surgery, mice received an intrathecal treatment of 100 or 300 nmol of SR9009. Withdrawal thresholds were then measured 1, 2, 3, 4, 5 and 24 hours post-injection. In paclitaxel mice, 14 days following the injection (6 days following the last injection), mice received an intrathecal treatment of 100 or 300 nmol of SR9009. Withdrawal thresholds were then measured 1, 2, 3, 6 and 24 hours post-injection. In diabetic mice, 21 days following the injection of streptozotocin, mice received an intrathecal treatment of 100 or 300 nmol of SR9009. Withdrawal thresholds were then measured 1, 2, 3, 6 and 24 hours post-injection.

Immunohistochemistry

Tissue sections of spinal dorsal horn from at least 3 mice of each treatment were used for immunohistochemistry. Thirty minutes after intrathecal administration of

SR9009, mice were further intrathecally injected of LPS. Fourteen days following PSNL, SR9009 was intrathecally injected. Then, after 3 hours, mice were anesthetized with isoflurane (induction; 5%, maintenance; 2-3%) and sodium pentobarbital (50 mg/kg, i.p.). Mice were transcardially perfused with 50 ml of saline followed by 100 ml of freshly prepared 4% (w/v) paraformaldehyde in 0.1 M phosphate buffer (pH = 7.4). The spinal tissues were quickly removed and postfixed in 4% paraformaldehyde in 0.1 M phosphate buffer for three days at 4°C and then cryoprotected overnight in 30% (w/v) sucrose in 0.1 M phosphate buffer at 4°C. Tissues were embedded in Tissue-Tek OCT compound 4583 (Sakura Finetech, Tokyo, Japan) and frozen in liquid nitrogen, cut serially (20 μm thickness) in a cryostat, and collected onto glass slides. After slides were dried at room temperature, tissue sections were processed for double-labeling immunohistochemistry. Tissue sections were rinsed with phosphate-buffered saline, incubated in a blocking solution of 10% goat serum, 3% bovine serum albumin, 0.1% Triton X and 0.05% Tween-20 in phosphate-buffered saline for 2 hours at room temperature, and then incubated with rabbit anti-glial fibrillary acidic protein (GFAP) antibody (1:1,000, GTX72747, GeneTex Inc., Irvine, CA, USA). Tissues were incubated in primary antibodies for 72 hours at 4°C, followed by corresponding secondary antibodies conjugated with Alexa Fluor® 488 (1:500) for 2 hours at 4°C in a dark chamber. The sections were then

extensively washed in phosphate-buffered saline and coverslipped. Sections were examined with a BZ-9000 Biorevo all-in-one fluorescence microscope (Keyence, Elmwood Park, NJ, USA).

Statistical analysis

Data are expressed as the mean±SEM of at least three independent determinations. The effects of drug treatment on mRNA and protein levels were performed using a one-way analysis of variance (ANOVA) with a pairwise comparison by the Tukey-Kramer method. Comparisons between two groups were performed using Student's t-test. Possible interactions between treatment over time on mechanical hypersensitivity were analyzed by two-way repeated-measures ANOVA, followed by the Tukey-Kramer method for post hoc comparisons. Differences were considered to be significant when the P value was less than 0.05.

Results

REV-ERBs agonists block LPS-induced production of pronociceptive molecules in cultured spinal astrocytes

Treatment of cultured spinal astrocytes with LPS markedly upregulated mRNA expression of pro-nociceptive molecules, including IL-1β, IL-6, MMP-9 and CCL2 (Fig. 1a-1d). Induction of IL-β mRNA expression was observed 1 hour, peaked 6 hours and declined 24 hours after treatment with LPS (Fig. 1a). The inhibitory effect of a specific REV-ERBs agonist SR9009 on LPS-induced IL-β mRNA expression was observed beginning 1 hour after treatment with LPS, and this effect lasted over the 24 hours incubation period (Fig. 1a). Although LPS-induced IL-6 mRNA expression was also observed 1 hour after LPS incubation, induction of IL-6 mRNA was significantly prevented by pretreatment with SR9009 at 6 and 24 hours (Fig. 1b). MMP-9 mRNA expression was significantly induced 3 hours after LPS treatment, and inhibitory effect of SR9009 on the MMP-9 mRNA expression was also observed at the same time and this effect lasted 24 hours (Fig. 1c). Induction of CCL2 mRNA was observed 1 hour after LPS treatment--SR9009 had no effect on LPS-induced CCL2 mRNA expression (Fig. 1d). Incubation of cultured spinal astrocytes with 10 μM of SR9009 alone did not significantly affect mRNA expression of pronociceptive molecules (Fig. 1). Pretreatment with SR9009 (3, 5 and 10 μM) significantly suppressed the stimulatory

effects of LPS on IL-1β mRNA, IL-6 mRNA and MMP-9 mRNA in a concentration-dependent manner (Fig. 2a-2c). Although SR9009 slightly inhibited LPS-induced CCL2 mRNA expression, this effect was not statistically significant (Fig. 2d). Furthermore, pretreatment with 10 and 20 μM of GSK4112, also a REV-ERB agonist, significantly suppressed LPS-induced mRNA expression of IL-1β, IL-6, MMP-9, but not CCL2 (Fig. 3a-3d). Incubation of cultured spinal astrocytes with 20 μM of GSK4112 alone did not significantly affect mRNA expression of pronociceptive molecules (Fig. 3). In addition, pretreatment with SR9009 also significantly blocked TNF-induced mRNA expression of IL-1β, IL-6 and MMP-9 (Fig. 4a-4c). In TNF-treated cells, similar to that observed following LPS treatment, SR9009 showed a trend towards inhibition of CCL2 mRNA expression, which was not statistically significant (Fig. 4d).

SR9009 inhibited LPS-induced protein expression of IL-1β, IL-6, CCL2 and MMP-9. Treatment with SR9009 (10 μM) significantly inhibited LPS-induced production of IL-1β, IL-6, but not CCL2 (Fig. 5a-5c). Furthermore, gelatin zymography showed that stimulation with LPS increased the activity of MMP-9 released into the cultured medium, and this effect was significantly blocked by pretreatment with SR9009 (Fig. 5d). Incubation of cultured spinal astrocytes with 10 μM of SR9009 alone did not significantly affect protein expression of pronociceptive molecules (Fig. 5a-5d).

As mentioned earlier, cultured spinal astrocytes express both Rev-erbα mRNA and Rev-erbβ mRNA (Morioka et al., 2016b), and SR9009 acts on both types of REV-ERBs with almost equal affinity (Solt et al., 2012). Thus, siRNA was used to inhibit expression of Rev-erbα mRNA and Rev-erbβ. As shown in Fig. 6a, the expression of both Rev-erbα mRNA and Rev-erbβ mRNA in cultured spinal astrocytes was significantly reduced after 48 hours of incubation with both siRNAs. Although significant inhibition by SR9009 on LPS-induced expression of IL-1β mRNA and MMP-9 mRNA was observed following knockdown of both Rev-erbs, the inhibitory effects of SR9009 were significantly reduced (Fig. 6b, 6d). Significant knockdown of both Rev-erbs mRNA almost completely reversed inhibitory effect of SR9009 on LPS-induced IL-6 mRNA expression (Fig. 6c). Thus, these results demonstrate that stimulation of REV-ERBs prevent the expression of pro-nociceptive molecules in spinal astrocytes.

Histone deacetylase 3 is a crucial mediator of the inhibitory effects of REV-ERBs on LPS-induced mRNA upregulation of IL-1β and IL-6, but not MMP-9, in cultured spinal astrocytes

Previous studies have demonstrated that REV-ERBs repress gene transcription through recruitment of nuclear receptor corepressor 1 (NCoR1) and HDAC3. Thus,

astrocytes were pretreated with the HDAC3 inhibitor RGFP966. RGFP966 (2 μM) reversed the inhibitory effect of SR9009 on LPS-induced expression of IL-1β mRNA and IL-6 mRNA (Fig. 7a, 7b). However, pretreatment with RGFP966 did not reverse LPS-induced expression of MMP-9 mRNA (Fig. 7c). Treatment with RGFP966 alone, without LPS and SR9009, did not affect IL-1β, IL-6 and MMP-9 mRNA expression. These results indicate that HDAC3 is necessary in the inhibitory effect of REV-ERBs on inducing IL-1β and IL-6 transcription with LPS. However, in the case of LPS-induced MMP-9 transcription, molecular mechanisms other than HDAC3 could be involved in the inhibitory effect of REV-ERB.

Stimulation of spinal REV-ERBs with specific agonists prevents LPS-induced mechanical hypersensitivity through downregulation of pronociceptive molecules

Potential antinociceptive effects of the activation of spinal REV-ERBs on LPS-induced hind paw mechanical hypersensitivity were examined. Intrathecal treatment with LPS induced significant mechanical hypersensitivity beginning 1 hour after injection, and lasted for as long as 24 hours after injection (Fig. 8). Intrathecal pretreatment with either SR9009 (100 and 300 nmol) or GSK4112 (100 nmol) prevented the onset of LPS-induced mechanical hypersensitivity (Fig. 7a; LPS versus

LPS+SR9009 100 nmol; $F_{1,144}$=15.3, P<0.001, interaction effect, $F_{1,144}$=3.36, P=0.00669, LPS versus LPS+SR9009 300 nmol; $F_{1,159}$=47.4, P<0.001, interaction effect, $F_{1,159}$=6.00, P<0.001, LPS versus LPS+GSK4112 100 nmol; $F_{1,127}$=14.5, P<0.001, interaction effect, $F_{1,127}$=5.17, P<0.001). Treatment with SR9009 alone had no effect on withdrawal thresholds of saline-treated mice (Fig. 8).

The effect of SR9009 on the expression of IL-1β, IL-6 and MMP-9 in spinal dorsal horn of mice following intrathecal treatment with LPS was examined. As the current study showed that antinociception with SR9009 was at least observed between 2-6 hours following administration of LPS, the effect of SR9009 on pronociceptive molecules expression was examined 3 hours after intrathecal treatment with LPS. The expression of both IL-1β and IL-6 mRNA was significantly increased in spinal dorsal horn following LPS treatment (Fig. 9a and 9b). Intrathecal pretreatment with SR9009 (100 and 300 nmol) significantly reduced both IL-1β and IL-6 mRNA expression in mice spinal dorsal horn treated with LPS (Fig. 9a and 9b). Intrathecal pretreatment with SR9009 alone did not change either IL-1β or IL-6 mRNA expression (Fig. 9a and 9b). In contrast to in vitro findings, intrathecal treatment with LPS did not significantly induce MMP-9 mRNA expression. Intrathecal SR9009 treatment in mice either with or without intrathecal LPS treatment did not affect MMP-9 mRNA expression (Fig. 9c).

Intrathecal treatment with SR9009 prevents LPS-induced GFAP expression in spinal dorsal horn

An increase of GFAP immunoreactivity, a cellular marker for astrocytes, was observed in the spinal dorsal horn 3 hours following intrathecal injection of LPS, indicating the presence of activated astrocytes. Intrathecal saline injection did not change GFAP expression. Mice were intrathecally pretreated with SR9009 (300 nmol) and 30 min later were intrathecally injected with LPS. SR9009 prevented LPS-induced GFAP expression in spinal dorsal horn (Fig. 10). The findings suggest that activation of REV-ERBs prevents astrocytic activation.

Effect of SR9009 on mechanical hypersensitivity in mouse models of inflammatory and neuropathic pain

The effect of SR9009 on CFA-induced peripheral inflammatory pain was investigated (Fig. 11a). After 7 days, intraplantar injection of CFA significantly decreased withdrawal thresholds to mechanical stimuli, indicating mechanical hypersensitivity (Fig. 11a). Intrathecal treatment with SR9009 (300 nmol) significantly ameliorated CFA-induced mechanical hypersensitivity (CFA versus CFA+SR9009 300 nmol; $F_{1,108}$=34.2, P<0.001, interaction effect, $F_{1,108}$=4.03, P=0.00215). Antinociceptive effect of SR9009 was observed beginning 2 hours after injection, and sustained for at

least 3 hours after injection (Fig. 11a). Treatment of saline-treated mice with SR9009 had no effect on withdrawal thresholds (Fig. 11a).

A potential antinociceptive effect of SR9009 on various types of neuropathic pain (PSNL, paclitaxel and streptozotocin) was examined. Fourteen days after surgery, intrathecal injection of SR9009 significantly reversed mechanical hypersensitivity in a dose-dependent manner in PSNL mice (Fig. 11b; PSNL versus PSNL+SR9009 100 nmol; $F_{1,155}$=42.5, P<0.001, interaction effect, $F_{1,155}$=12.0, P<0.001, PSNL versus PSNL+SR9009 300 nmol; $F_{1,151}$=74.3, P<0.001, interaction effect, $F_{1,151}$=14.1, P<0.001). The antinociceptive effect of 300 nmol SR9009 was observed beginning 2 hours after injection and sustained for at least 3 hours after injection. Intrathecal injection of SR9009 (100 nmol) also significantly increased withdrawal thresholds to mechanical stimuli for about 3 hours after injection in PSNL mice (Fig. 11b). Intrathecal treatment with SR9009 (300 nmol) in sham-operated mice had no effect on withdrawal thresholds (Fig. 11b).

Significant mechanical hypersensitivity was observed 14 days following the first injection of paclitaxel (Fig. 11c). Intrathecal treatment with SR9009 significantly ameliorated paclitaxel-induced mechanical hypersensitivity (Fig. 11c; paclitaxel versus paclitaxel+SR9009 100 nmol; $F_{1,72}$=117.94, P<0.001, interaction effect, $F_{1,72}$=9.00, P<0.001). The antinociceptive effect of 100 nmol SR9009 was significant

beginning 1 hour after injection and lasted for at least 6 hours after injection (Fig. 11c). By contrast, the antinociceptive effect of 300 nmol SR9009 was observed 2 hours after injection (Fig. 11c). Intrathecal injection of SR9009 (300 nmol) in vehicle-treated mice had no effect on withdrawal thresholds (Fig. 11c).

Significant mechanical hypersensitivity was observed three weeks following the injection of streptozotocin (Fig. 11d). Intrathecal treatment with 300 nmol of SR9009 significantly ameliorated streptozotocin-induced mechanical hypersensitivity (Fig. 11d; streptozotocin versus streptozotocin+SR9009 300 nmol; $F_{1,66}$=82.9, P<0.001, interaction effect, $F_{1,66}$=22.2, P<0.001). The antinociceptive effect of 300 nmol SR9009 was observed beginning 2 hours after injection, and lasted for at least 3 hours after injection (Fig. 11d). By contrast, no antinociceptive effect was observed with 100 nmol SR9009 (Fig. 11d). Intrathecal injection of SR9009 (300 nmol) in vehicle-treated mice had no effect on withdrawal thresholds (Fig. 11d).

Intrathecal treatment with SR9009 reverses upregulation of GFAP in spinal dorsal horn following sciatic nerve injury

Fourteen days following PSNL, during the period of significant mechanical hypersensitivity, spinal dorsal horn GFAP expression was significantly increased compared than that of sham mice (Fig. 12a and 12b). Treatment with SR9009 (300

nmol) significantly suppressed PSNL-induced GFAP expression in spinal dorsal horn (Fig. 12a and 12b). Treatment with vehicle or SR9009 alone had no effect on GFAP expression in spinal dorsal horn of sham mice (Fig. 12a and 12b).

Discussion

The current study examined whether REV-ERBs could be targeted to relieve pain in various chronic pain states. In the current study, activation of cultured spinal astrocytes' REV-ERBs prevented the expression of pronociceptive molecules by an inflammatory stimulus. During the maintenance phase of chronic pain, pronociceptive molecules produced by activated spinal astrocytes have a crucial role in mediating nociceptive hypersensitivity. In mice, activation of spinal REV-ERBs prevented LPS-induced mechanical hypersensitivity through the downregulation of IL-1β and IL-6 expression in spinal dorsal horn. Furthermore, activation of spinal REV-ERBs in mice reversed inflammatory and neuropathic mechanical hypersensitivity. In addition, stimulation of spinal REV-ERBs blocked upregulation of astrocytic activation marker protein GFAP in spinal dorsal horn of inflammatory and neuropathic pain model mice. Thus, the current findings suggest that astrocytic REV-ERBs could be crucial in the regulation of nociceptive transduction through the inhibition of the production of pronociceptive molecules.

Significant involvement of REV-ERBs in the regulation of the response to inflammatory stimulation has been previously reported. Activation of REV-ERBs suppressed TNF-induced expression of CCL2 mRNA and MMP-9 mRNA, but not IL-6 mRNA and inducible nitric oxide synthase mRNA, in C6 glioma cells (Morioka et al.,

2016b). REV-ERBs appear to modulate the expression of proinflammatory molecules of various immune cells. Co-treatment with SR9009 blocked LPS and interferon-γ-induced expression of IL-6 mRNA and IL-1β mRNA in mouse bone marrow-derived macrophages and activation REV-ERBα blocked IL-6 and CCL2 expression in mouse peritoneal macrophage (Sato et al., 2014; Sitaula et al., 2015). Mutation of REV-ERBs in bronchial epithelia augmented inflammatory responses and chemokine production, demonstrating the importance of activated REV-ERBs in the response to inflammatory stimuli (Pariollaud et al., 2018). Although *Rev-erb* mRNA expression has been observed in cultured spinal astrocytes (Morioka et al., 2016b), there are no reports regarding the function of REV-ERB subtypes in spinal astrocytes.

The current study demonstrated that activation of REV-ERBs expressed on cultured spinal astrocytes suppressed LPS-induced expression of IL-1β, IL-6 and MMP-9. The proinflammatory cytokine TNF, which is mainly produced from activated microglia, has been shown to induce the production of pronociceptive molecules and evoke mechanical hypersensitivity, possibly through the activation of spinal astrocytes (Grace et al., 2014; Morioka et al., 2014). In the current study, activation of spinal astrocytic REV-ERBs also prevented TNF-induced expression of IL-1β, IL-6 and MMP-9. Thus, it is possible that REV-ERBs could suppress activation of astrocytes regardless of the inflammatory stimulus. REV-ERBs activation partially inhibited

induction of CCL2 expression, indicating that REV-ERBs play a minor role in the expression of this pronociceptive molecule and further suggests that REV-ERBs modulate the expression of many but not all pronociceptive molecules. The inhibitory effects of REV-ERBs agonist SR9009 can be attributed to direct stimulation of REV-ERBs, as knockdown of both subtypes of REV-ERB by RNA interference led to a lack of efficacy of the agonist and SR9009 has no significant cross-activity against other members of the nuclear receptor superfamily (Solt et al., 2012). Together, these findings indicate that activation of spinal astrocytic REV-ERBs have a significant role in mediating antinociception.

REV-ERBs bind to retinoic acid receptor-related orphan receptors (RORs) element (RORE) and compete in binding of positive transcriptional factor RORs (Kojetin and Burris, 2014; Sato et al., 2014). Furthermore, it has been shown that the HDAC3-dependent transcriptional inhibition by REV-ERB activation could be mediated through the modulation of response elements different from that of the RORE motif (Zhang et al., 2015). These are the potential mechanism mediating REV-ERBs inhibition of transcription. The current study showed that HDAC3 activity is crucial in the inhibitory effects of REV-ERBs on LPS-induced expression of IL-1β and IL-6, but not MMP-9. Thus, it is possible that the effect of REV-ERBs on MMP-9 in spinal astrocytes could be regulated by a RORs-dependent mechanism. By contrast, a

previous study demonstrated that the inhibitory effect of REV-ERBs on MMP-9 induction is dependent on HDAC3 in C6 glioma cells (Morioka et al., 2016b). Thus, these findings suggest that a REV-ERBs-mediated inhibitory mechanism could be dependent whether a ROR element or HDAC3-acting sites exist in the promoter regions of the target gene in different cell types.

Activated spinal astrocytes have a key role in the maintenance of nociceptive hypersensitivity during the chronic pain state, so targeting astrocytic activity could lead to significant analgesia. While there are a number of mechanistic distinctions between inflammatory and neuropathic pain, it has been found that activation of spinal astrocytes is crucial across these models (Deng et al., 2017; Morioka et al., 2015; Qian et al., 2016). In the case of paclitaxel-induced neuropathy and PSNL, mechanical hypersensitivity appears to be mainly mediated through activation of spinal dorsal horn astrocytes and not microglia (Li et al., 2014; Morioka et al., 2015; Zhang et al., 2012a). Intrathecal LPS-induced mechanical hypersensitivity is likely due to activation of astrocytes in spinal dorsal horn (Lu et al., 2015; Saito et al., 2010; Zhao et al., 2014) and in the current study activation of REV-ERBs reduced both LPS- and PSNL-induced GFAP expression in spinal dorsal horn as well as suppressed mechanical hypersensitivity in both pain model mice. It is possible, then, that the antinociceptive effect of REV-ERBs activation observed across the current set of

chronic pain models could be mediated, in part, by suppression of astrocytic activation.

While astrocytic functional status, such as GFAP immunoreactivity, was not directly assessed in the neuropathic and inflammatory pain models in the current study, reduced astrocytic functioning following REV-ERBs activation was inferred by reduced production of pronociceptive cytokines (Grace et al., 2014; Hansen and Malcangio, 2013; Nakagawa and Kaneko, 2010). The current study confirmed previous finding, in that stimulation of spinal dorsal horn astrocytes in vivo with LPS upregulated pronociceptive molecules, including IL-1β and IL-6, (Lu et al., 2015; Zhao et al., 2014). Previous studies also showed that these molecules mediate LPS-induced hypersensitivity (Loram et al., 2011; Zhu et al., 2014). In the current study, upregulation of IL-1β and IL-6 was prevented and mechanical hypersensitivity was reduced with intrathecal treatment with a REV-ERB agonist. Thus, the decreased expression of pronociceptive molecules and decreased mechanical hypersensitivity observed following spinal REV-ERBs activation suggests decreased spinal astrocytic activation.

The inhibitory role of REV-ERBα in gene expression is well known. REV-ERBβ contributes to the regulation of genes involved in lipid and energy homeostasis in skeletal muscle cells (Ramakrishnan et al., 2005). Furthermore, several types of

tumor cell predominantly express REV-ERBβ, and genetic or pharmacological inhibition of REV-ERBβ sensitizes cancer cells to the cytotoxic reagent chloroquine, which suppresses autophagy (De Mei et al., 2015). In the current study, the inhibitory role of each REV-ERB on the expression of pronociceptive molecules was not clearly demarcated. Preliminary findings suggested that although knockdown of both REV-ERBs by RNA interference prevented SR9009-induced suppression of gene expression in cultured spinal astrocytes, knockdown of either REV-ERB alone did not (data not shown). Thus, each REV-ERB subtype could have a distinct function in regulating IL-6, IL-1β and MMP-9 transcription in spinal astrocytes.

A number of studies demonstrated that activation of REV-ERBs suppresses MMP-9 expression in various cell types (Lam et al., 2013; Morioka et al., 2016b; Song et al., 2018; Stujanna et al., 2017). Interestingly, in the current study, while in vitro astrocytic expression of MMP-9 mRNA increased following LPS treatment, spinal dorsal horn MMP-9 expression was not changed following intrathecal LPS treatment. Therefore, it is possible that MMP-9 might not be involved in LPS-induced nociceptive hypersensitivity in vivo. Alternatively, it is possible that MMP-9 is involved in late-stage maintenance of LPS-induced hypersensitivity, as the current study found peak in vitro expression of MMP-9 mRNA was later than that of IL-1β mRNA and IL-6 mRNA. In vivo findings in inflammatory and neuropathic pain models suggest that spinal MMP-9

is likely involved in late-stage maintenance of pain (Jiang et al., 2017; Kular et al., 2012). Although further investigation is needed, downregulation of MMP-9 could be one of the mechanisms underlying the antinociceptive effect of SR9009 and MMP-9 could be an important molecule mediating established nociceptive hypersensitivity across a variety of pain states.

While the current study confirms a role of spinal astrocytes in the maintenance of chronic pain, activated spinal microglial REV-ERBs could also have an antinociceptive function. Intrathecal injection of LPS activates both spinal dorsal horn microglia and astrocytes (Saito et al., 2010; Zhao et al., 2014; Zhu et al., 2014). Treatment of cultured mouse brain microglia with the REV-ERB agonist SR9011 suppressed LPS-induced IL-6 expression (Nakazato et al., 2017). Therefore, it is possible that spinal microglial REV-ERBs could modulate spinal IL-1β and IL-6 mRNA expression in the current study, thereby contributing to REV-ERB agonist-mediated antinociception observed in the current study. However, whether spinal microglial REV-ERBs regulate the expression of proinflammatory molecules is not unknown.

In conclusion, the current findings demonstrated that stimulation of spinal astrocytic REV-ERBs suppressed astrocytic functioning, as inferred by decreased production of pronociceptive molecules IL-1β and IL-6. Stimulation of spinal astrocytic REV-ERBs could be effective in a wide range of pain states as astrocytes have a key role in

mediating chronic pain, regardless of etiology. Therefore, targeting spinal astrocytic REV-ERBs could be a novel therapeutic strategy for ameliorating chronic pain.

Acknowledgements

This work was supported by Grant-in-Aid for Scientific Research (C) grant number 26460342, and grants from the Takeda Science Foundation, Suzuken Memorial Foundation, The Uehara Memorial Foundation and The Nakatomi Foundation. Experiments were carried out using equipment at the Analysis Center of Life Science, Hiroshima University and the Research Center for Molecular Medicine, Faculty of Medicine, Hiroshima University. We also thank Dr. Aldric T. Hama for his critical reading of the manuscript.

References

Abe, H., Hisaoka-Nakashima, K., Kajitani, N., Okada-Tsuchioka, M., Yano, R., Itagaki, K., Shibasaki, C., Morioka, N., Nakata, Y., Takebayashi, M., 2016. The expression of glial cell line-derived neurotrophic factor mRNA by antidepressants involves matrix metalloproteinase-9 activation in rat astroglial cells. Biochem Biophys Res Commun 479, 907-912.

Das, V., Kc, R., Li, X., Varma, D., Qiu, S., Kroin, J.S., Forsyth, C.B., Keshavarzian, A., van Wijnen, A.J., Park, T.J., Stein, G.S., O-Sullivan, I., Burris, T.P., Im, H.J., 2018. Pharmacological targeting of the mammalian clock reveals a novel analgesic for osteoarthritis-induced pain. Gene 655, 1-12.

De Mei, C., Ercolani, L., Parodi, C., Veronesi, M., Lo Vecchio, C., Bottegoni, G., Torrente, E., Scarpelli, R., Marotta, R., Ruffili, R., Mattioli, M., Reggiani, A., Wade, M., Grimaldi, B., 2015. Dual inhibition of REV-ERBβ and autophagy as a novel pharmacological approach to induce cytotoxicity in cancer cells. Oncogene 34, 2597-2608.

Deng, X.T., Wu, M.Z., Xu, N., Ma, P.C., Song, X.J., 2017. Activation of ephrinB-EphB receptor signalling in rat spinal cord contributes to maintenance of diabetic neuropathic pain. Eur J Pain 21, 278-288.

Ferreira, M.L., de Luca, K., 2017. Spinal pain and its impact on older people. Best Pract Res Clin Rheumatol 31, 192-202.

Gagliese, L., Gauthier, L.R., Narain, N., Freedman, T., 2017. Pain, aging and dementia: Towards a biopsychosocial model. Prog Neuropsychopharmacol Biol Psychiatry.

Gao, Y.J., Zhang, L., Samad, O.A., Suter, M.R., Yasuhiko, K., Xu, Z.Z., Park, J.Y., Lind, A.L., Ma, Q., Ji, R.R., 2009. JNK-induced MCP-1 production in spinal cord

astrocytes contributes to central sensitization and neuropathic pain. J Neurosci 29, 4096-4108.

Grace, P.M., Hutchinson, M.R., Maier, S.F., Watkins, L.R., 2014. Pathological pain and the neuroimmune interface. Nat Rev Immunol 14, 217-231.

Grant, D., Yin, L., Collins, J.L., Parks, D.J., Orband-Miller, L.A., Wisely, G.B., Joshi, S., Lazar, M.A., Willson, T.M., Zuercher, W.J., 2010. GSK4112, a small molecule chemical probe for the cell biology of the nuclear heme receptor Rev-erbα. ACS Chem Biol 5, 925-932.

Hansen, R.R., Malcangio, M., 2013. Astrocytes--multitaskers in chronic pain. Eur J Pharmacol 716, 120-128.

Ji, R.R., Chamessian, A., Zhang, Y.Q., 2016. Pain regulation by non-neuronal cells and inflammation. Science 354, 572-577.

Jiang, L., Pan, C.L., Wang, C.Y., Liu, B.Q., Han, Y., Hu, L., Liu, L., Yang, Y., Qu, J.W., Liu, W.T., 2017. Selective suppression of the JNK-MMP2/9 signal pathway by tetramethylpyrazine attenuates neuropathic pain in rats. J Neuroinflammation 14, 174.

Kojetin, D.J., Burris, T.P., 2014. REV-ERB and ROR nuclear receptors as drug targets. Nat Rev Drug Discov 13, 197-216.

Kular, L., Rivat, C., Lelongt, B., Calmel, C., Laurent, M., Pohl, M., Kitabgi, P., Melik-Parsadaniantz, S., Martinerie, C., 2012. NOV/CCN3 attenuates inflammatory pain through regulation of matrix metalloproteinases-2 and -9. J Neuroinflammation 9, 36.

Lam, M.T., Cho, H., Lesch, H.P., Gosselin, D., Heinz, S., Tanaka-Oishi, Y., Benner, C., Kaikkonen, M.U., Kim, A.S., Kosaka, M., Lee, C.Y., Watt, A., Grossman, T.R., Rosenfeld, M.G., Evans, R.M., Glass, C.K., 2013. Rev-Erbs repress macrophage gene expression by inhibiting enhancer-directed transcription. Nature 498, 511-515.

Lee, J., Ko, H.G., Kim, K., Kaang, B.K., 2016. Mildly Increased Mechanical Nociceptive Sensitivity in REV-ERBα Knock-out Mice. Exp Neurobiol 25, 342-346.

Li, Y., Zhang, H., Kosturakis, A.K., Jawad, A.B., Dougherty, P.M., 2014. Toll-like receptor 4 signaling contributes to Paclitaxel-induced peripheral neuropathy. J Pain 15, 712-725.

Loram, L.C., Taylor, F.R., Strand, K.A., Frank, M.G., Sholar, P., Harrison, J.A., Maier, S.F., Watkins, L.R., 2011. Prior exposure to glucocorticoids potentiates lipopolysaccharide induced mechanical allodynia and spinal neuroinflammation. Brain Behav Immun 25, 1408-1415.

Lu, Y., Cao, D.L., Jiang, B.C., Yang, T., Gao, Y.J., 2015. MicroRNA-146a-5p attenuates neuropathic pain via suppressing TRAF6 signaling in the spinal cord. Brain Behav Immun 49, 119-129.

Mika, J., Zychowska, M., Popiolek-Barczyk, K., Rojewska, E., Przewlocka, B., 2013. Importance of glial activation in neuropathic pain. Eur J Pharmacol 716, 106-119.

Morioka, N., Abe, H., Araki, R., Matsumoto, N., Zhang, F.F., Nakamura, Y., Hisaoka-Nakashima, K., Nakata, Y., 2014. A β1/2 adrenergic receptor-sensitive intracellular signaling pathway modulates CCL2 production in cultured spinal astrocytes. J Cell Physiol 229, 323-332.

Morioka, N., Fujii, S., Kondo, S., Zhang, F.F., Miyauchi, K., Nakamura, Y., Hisaoka-Nakashima, K., Nakata, Y., 2018. Downregulation of spinal astrocytic connexin43 leads to upregulation of interleukin-6 and cyclooxygenase-2 and mechanical hypersensitivity in mice. Glia 66, 428-444.

Morioka, N., Saeki, M., Sugimoto, T., Higuchi, T., Zhang, F.F., Nakamura, Y., Hisaoka-Nakashima, K., Nakata, Y., 2016a. Downregulation of the spinal dorsal horn clock gene Per1 expression leads to mechanical hypersensitivity via c-jun N-terminal kinase and CCL2 production in mice. Mol Cell Neurosci 72, 72-83.

Morioka, N., Tomori, M., Zhang, F.F., Saeki, M., Hisaoka-Nakashima, K., Nakata, Y., 2016b. Stimulation of nuclear receptor REV-ERBs regulates tumor necrosis factor-

induced expression of proinflammatory molecules in C6 astroglial cells. Biochem Biophys Res Commun 469, 151-157.

Morioka, N., Zhang, F.F., Nakamura, Y., Kitamura, T., Hisaoka-Nakashima, K., Nakata, Y., 2015. Tumor necrosis factor-mediated downregulation of spinal astrocytic connexin43 leads to increased glutamatergic neurotransmission and neuropathic pain in mice. Brain Behav Immun 49, 293-310.

Nakagawa, T., Kaneko, S., 2010. Spinal astrocytes as therapeutic targets for pathological pain. J Pharmacol Sci 114, 347-353.

Nakamura, Y., Morioka, N., Zhang, F.F., Hisaoka-Nakashima, K., Nakata, Y., 2015. Downregulation of connexin36 in mouse spinal dorsal horn neurons leads to mechanical allodynia. J Neurosci Res 93, 584-591.

Nakazato, R., Hotta, S., Yamada, D., Kou, M., Nakamura, S., Takahata, Y., Tei, H., Numano, R., Hida, A., Shimba, S., Mieda, M., Hinoi, E., Yoneda, Y., Takarada, T., 2017. The intrinsic microglial clock system regulates interleukin-6 expression. Glia 65, 198-208.

Pariollaud, M., Gibbs, J.E., Hopwood, T.W., Brown, S., Begley, N., Vonslow, R., Poolman, T., Guo, B., Saer, B., Jones, D.H., Tellam, J.P., Bresciani, S., Tomkinson, N.C., Wojno-Picon, J., Cooper, A.W., Daniels, D.A., Trump, R.P., Grant, D., Zuercher, W., Willson, T.M., MacDonald, A.S., Bolognese, B., Podolin, P.L., Sanchez, Y., Loudon, A.S., Ray, D.W., 2018. Circadian clock component REV-ERBα controls homeostatic regulation of pulmonary inflammation. J Clin Invest 128, 2281-2296.

Qian, B., Li, F., Zhao, L.X., Dong, Y.L., Gao, Y.J., Zhang, Z.J., 2016. Ligustilide Ameliorates Inflammatory Pain and Inhibits TLR4 Upregulation in Spinal Astrocytes Following Complete Freund's Adjuvant Peripheral Injection. Cell Mol Neurobiol 36, 143-149.

Ramakrishnan, S.N., Lau, P., Burke, L.J., Muscat, G.E., 2005. Rev-erbbeta regulates

the expression of genes involved in lipid absorption in skeletal muscle cells: evidence for cross-talk between orphan nuclear receptors and myokines. J Biol Chem 280, 8651-8659.

Saito, O., Svensson, C.I., Buczynski, M.W., Wegner, K., Hua, X.Y., Codeluppi, S., Schaloske, R.H., Deems, R.A., Dennis, E.A., Yaksh, T.L., 2010. Spinal glial TLR4-mediated nociception and production of prostaglandin E(2) and TNF. Br J Pharmacol 160, 1754-1764.

Sato, S., Sakurai, T., Ogasawara, J., Takahashi, M., Izawa, T., Imaizumi, K., Taniguchi, N., Ohno, H., Kizaki, T., 2014. A circadian clock gene, Rev-erbα, modulates the inflammatory function of macrophages through the negative regulation of Ccl2 expression. J Immunol 192, 407-417.

Shibata, K., Sugawara, T., Fujishita, K., Shinozaki, Y., Matsukawa, T., Suzuki, T., Koizumi, S., 2011. The astrocyte-targeted therapy by Bushi for the neuropathic pain in mice. PLoS One 6, e23510.

Sitaula, S., Billon, C., Kamenecka, T.M., Solt, L.A., Burris, T.P., 2015. Suppression of atherosclerosis by synthetic REV-ERB agonist. Biochem Biophys Res Commun 460, 566-571.

Solt, L.A., Wang, Y., Banerjee, S., Hughes, T., Kojetin, D.J., Lundasen, T., Shin, Y., Liu, J., Cameron, M.D., Noel, R., Yoo, S.H., Takahashi, J.S., Butler, A.A., Kamenecka, T.M., Burris, T.P., 2012. Regulation of circadian behaviour and metabolism by synthetic REV-ERB agonists. Nature 485, 62-68.

Song, C., Tan, P., Zhang, Z., Wu, W., Dong, Y., Zhao, L., Liu, H., Guan, H., Li, F., 2018. REV-ERB agonism suppresses osteoclastogenesis and prevents ovariectomy-induced bone loss partially via FABP4 upregulation. FASEB J 32, 3215-3228.

Stujanna, E.N., Murakoshi, N., Tajiri, K., Xu, D., Kimura, T., Qin, R., Feng, D., Yonebayashi, S., Ogura, Y., Yamagami, F., Sato, A., Nogami, A., Aonuma, K., 2017.

Rev-erb agonist improves adverse cardiac remodeling and survival in myocardial infarction through an anti-inflammatory mechanism. PLoS One 12, e0189330.

Sulli, G., Rommel, A., Wang, X., Kolar, M.J., Puca, F., Saghatelian, A., Plikus, M.V., Verma, I.M., Panda, S., 2018. Pharmacological activation of REV-ERBs is lethal in cancer and oncogene-induced senescence. Nature 553, 351-355.

Yin, L., Lazar, M.A., 2005. The orphan nuclear receptor Rev-erbalpha recruits the N-CoR/histone deacetylase 3 corepressor to regulate the circadian Bmal1 gene. Mol Endocrinol 19, 1452-1459.

Zhang, F.F., Morioka, N., Harano, S., Nakamura, Y., Liu, K., Nishibori, M., Hisaoka-Nakashima, K., Nakata, Y., 2016. Perineural expression of high-mobility group box-1 contributes to long-lasting mechanical hypersensitivity via matrix metalloprotease-9 up-regulation in mice with painful peripheral neuropathy. J Neurochem 136, 837-850.

Zhang, H., Yoon, S.Y., Dougherty, P.M., 2012a. Evidence that spinal astrocytes but not microglia contribute to the pathogenesis of Paclitaxel-induced painful neuropathy. J Pain 13, 293-303.

Zhang, X., Xu, Y., Wang, J., Zhou, Q., Pu, S., Jiang, W., Du, D., 2012b. The effect of intrathecal administration of glial activation inhibitors on dorsal horn BDNF overexpression and hind paw mechanical allodynia in spinal nerve ligated rats. J Neural Transm 119, 329-336.

Zhang, Y., Fang, B., Emmett, M.J., Damle, M., Sun, Z., Feng, D., Armour, S.M., Remsberg, J.R., Jager, J., Soccio, R.E., Steger, D.J., Lazar, M.A., 2015. GENE REGULATION. Discrete functions of nuclear receptor Rev-erbα couple metabolism to the clock. Science 348, 1488-1492.

Zhao, L.X., Jiang, B.C., Wu, X.B., Cao, D.L., Gao, Y.J., 2014. Ligustilide attenuates inflammatory pain via inhibition of NFκB-mediated chemokines production in spinal astrocytes. Eur J Neurosci 39, 1391-1402.

Zhu, M.D., Zhao, L.X., Wang, X.T., Gao, Y.J., Zhang, Z.J., 2014. Ligustilide inhibits microglia-mediated proinflammatory cytokines production and inflammatory pain. Brain Res Bull 109, 54-60.

Zhuang, Z.Y., Gerner, P., Woolf, C.J., Ji, R.R., 2005. ERK is sequentially activated in neurons, microglia, and astrocytes by spinal nerve ligation and contributes to mechanical allodynia in this neuropathic pain model. Pain 114, 149-159.

Figure Legends

Figure 1. Suppressive effect of SR9009 on LPS-induced upregulation of IL-1β mRNA (a), IL-6 mRNA (b), MMP-9 mRNA (c) and CCL2 mRNA (d) expression over time in cultured spinal astrocytes. After treatment with REV-ERB agonist SR9009 (10 μM) for 30 min, cells were then stimulated with LPS (10 ng/ml) for time periods indicated (1, 3, 6 and 24 hours). Then, expression levels of each mRNA were determined. Data are expressed as ratio of vehicle at each corresponding time point, and represent the mean± SEM for five independent experiments. *P<0.05, **P<0.01 vs. vehicle treatment. †P<0.05, ††P<0.01 vs. LPS treatment alone.

Figure 2. Effect of SR9009 on LPS-induced upregulation of IL-1β mRNA (a), IL-6 mRNA (b), MMP-9 mRNA (c) and CCL2 mRNA (d) expression in cultured spinal astrocytes. After treatment with REV-ERB agonist SR9009 (3, 5 or 10 μM) for 30 min, cells were then stimulated with LPS (10 ng/ml) for 24 hours. Cells were also treated with SR9009 in the absence of LPS. Data represent the mean±SEM for six to nine independent experiments. **P<0.01 vs. vehicle treatment. ††P<0.01 vs. LPS treatment alone.

Figure 3. Effect of GSK4112 on LPS-induced upregulation of IL-1β mRNA (a), IL-6

mRNA (b), MMP-9 mRNA (c) and CCL2 mRNA (d) expression in cultured spinal astrocytes. After treatment with REV-ERB agonist GSK4112 (10 or 20 μM) for 30 min, cells were then stimulated with LPS (10 ng/ml) for 24 hours. Cells were also treated with GSK4112 in the absence of LPS. Data represent the mean ± SEM for five independent experiments. **P<0.01 vs. vehicle treatment. †P<0.05, ††P<0.01 vs. LPS treatment alone.

Figure 4. Effect of SR9009 on TNF-induced upregulation of IL-1β mRNA (a), IL-6 mRNA (b), MMP-9 mRNA (c) and CCL2 mRNA (d) expression in cultured spinal astrocytes. After treatment with SR9009 (3 or 5 μM) for 30 min, cells were then stimulated with TNF (10 ng/ml) for 24 hours. Cells were also treated with SR9009 in the absence of TNF. Data represent the mean ± SEM for five independent experiments. **P<0.01 vs. vehicle treatment. †P<0.05, ††P<0.01 vs. LPS treatment alone.

Figure 5. Effects of SR9009 on LPS-induced upregulation of proinflammatory molecule protein expression in cultured spinal astrocytes. Effects of SR9009 on LPS-induced expression of IL-1β (a), IL-6 (b) and CCL2 (c) protein in cultured spinal astrocytes. After treatment with SR9009 (10 μM) for 30 min, cells were then

stimulated with LPS (10 ng/ml) for 24 hours. The expression levels of these proteins were measured by ELISA. Data represent the mean ± SEM for four independent experiments. *P<0.05, **P<0.01 vs. vehicle treatment. †P<0.05, ††P<0.01 vs. LPS treatment alone. (d) Effects of SR9009 on LPS-induced MMP-9 activity in cultured spinal astrocytes. After treatment with SR9009 (10 μM) for 30 min, cells were then stimulated with LPS (10 ng/ml) for 24 hours. The activity of MMP-9 was measured by zymography. The upper photograph is a representative zymography of MMP-9. Quantitative graph are shown below. Data represent the mean ± SEM for six independent experiments. **P<0.01 vs. vehicle treatment. †P<0.05 vs. LPS treatment alone.

Figure 6. REV-ERB activation is involved in the suppressed expression of proinflammatory molecules in cultured spinal astrocytes. (a) Silencing of Rev-erbα and Rev-erbβ expression in cultured spinal astrocytes. Cells were transfected with either non-targeting siRNA or a combination of Rev-erbα- and Rev-erbβ-tageting silencing interfering RNA (Rev-erbα/β siRNA). After 24 hours, Rev-erb mRNA expression levels were examined. Data represent the mean ± SEM for five independent experiments. **P<0.01 vs. non-targeting siRNA treatment. Downregulation of Rev-erbs expression by siRNA prevented the inhibitory effect of

SR9009 on LPS-induced upregulation of IL-1β mRNA (b), IL-6 mRNA (c) and MMP-9 mRNA (d) expression in cultured spinal astrocytes. After transfection with either non-targeting siRNA or a combination of Rev-erbα- and Rev-erbβ-targeting siRNA for 24 hours, astrocytes were treated with 5 μM of SR9009 for 30 min. Cells were then treated with 10 ng/ml of LPS for 24 hours. Data represent the mean±SEM for five independent experiments. **P<0.01 vs. LPS alone at each siRNA treatment. †P<0.05, ††P<0.01 vs. LPS + SR9009 at non-targeting siRNA.

Figure 7. HDAC3 is involved in REV-ERB-mediated inhibition of IL-1β mRNA and IL-6 mRNA expression, but not MMP-9 mRNA expression. After treatment with the selective HDAC3 inhibitor RGFP966 (2 μM) for 30 min, cells were incubated with SR9009 (5 μM) for 30 min and then LPS (10 ng/ml) for 24 hours. Cells were also incubated in RGFP966 (2 μM) in the absence of SR9009 and LPS. Expression levels of L-1β mRNA (a), IL-6 mRNA (b) and MMP-9 mRNA (c) relative to LPS-treated astrocytes are shown. Data represent the mean±SEM for five to eight independent experiments. **P<0.01 vs. vehicle treatment. †P<0.05, ††P<0.01 vs. LPS treatment alone. ##P<0.01 vs. SR9009+LPS treatment.

Figure 8. REV-ERBs agonists prevent mechanical hypersensitivity of mice intrathecally injected with LPS. One hour after intrathecal treatment with either SR9009 (100 or 300 nmol), GSK4112 (100 nmol) or DMSO, either LPS (0.1 μg) or saline was intrathecally injected and hind paw withdrawal thresholds were assessed over time. n=10-13/group. Data represent the mean ± SEM. *P<0.05, **P<0.01 vs. saline-injected mice with DMSO at the corresponding time point. †P<0.05, ††P<0.01 vs. LPS-injected mice with DMSO at the corresponding time point.

Figure 9. Activation of REV-ERBs reduces expression of IL-1β mRNA and IL-6 mRNA in spinal dorsal horn of mice intrathecally injected with LPS. Thirty minutes after intrathecal treatment with either SR9009 (100 or 300 nmol) or DMSO, either LPS (0.1 μg) or saline was intrathecally injected. Three hours later, spinal dorsal horn expression levels of L-1β mRNA (a), IL-6 mRNA (b) and MMP-9 mRNA (c) were measured. n=7-10/group. Data represent the mean ± SEM. **P<0.01 vs. saline-injected mice with DMSO. †P<0.05, ††P<0.01 vs. LPS-injected mice with DMSO.

Figure 10. Activation of REV-ERB prevents GFAP expression in spinal dorsal horn of mice intrathecally injected with LPS. (a) Thirty minutes after intrathecal treatment with either SR9009 (300 nmol) or DMSO, either LPS (0.1 μg) or saline was intrathecally

injected. Spinal dorsal horn was harvested 3 hours after LPS injection. Magnified photomicrographs of the white boxed areas are to the right. Scar bar=100 μm. (b) Quantitative analysis of expression of GFAP in spinal dorsal horn after injection of drugs described above at 3 hours following LPS injection. Data indicate mean ratio of sum of GFAP immunofluorescence intensity in each mice, and expressed as mean ± SEM for six to eight mice. **P<0.01 vs. saline-injected mice with DMSO. †P<0.05 vs. LPS-injected mice with DMSO.

Figure 11. Activation of REV-ERBs ameliorates mechanical hypersensitivity in mouse models of both inflammatory and neuropathic pain. a) Seven days after intraplantar treatment with either CFA or saline, either SR9009 (100 or 300 nmol) or DMSO was intrathecally injected and hind paw withdrawal thresholds were assessed over time. n=10/group. Data represent the mean ± SEM. **P<0.01 vs. saline-injected mice with DMSO at the corresponding time point. ††P<0.01 vs. CFA-injected mice with DMSO at the corresponding time point. b) Fourteen days after sciatic nerve injury, either SR9009 (100 or 300 nmol) or DMSO was intrathecally injected and hind paw withdrawal thresholds were assessed over time. n=11-14/group. Data represent the mean ± SEM. **P<0.01 vs. sham mice with vehicle at the corresponding time point. †P<0.05, ††P<0.01 vs. PSNL mice with vehicle at the corresponding time point. c)

Fourteen days after intraperitoneal treatment with either paclitaxel (PTX) or vehicle (6 days after last injection), either SR9009 (100 or 300 nmol) or DMSO was intrathecally injected and hind paw withdrawal thresholds were assessed over time. n=5-8/group. Data represent the mean ± SEM. *P<0.05, **P<0.01 vs. vehicle-injected mice with DMSO at the corresponding time point. †P<0.05, ††P<0.01 vs. PTX-injected mice with DMSO at the corresponding time point. d) Twenty one days after intraperitoneal treatment with either streptozotocin (STZ) or saline, either SR9009 (100 or 300 nmol) or DMSO was intrathecally injected and hind paw withdrawal thresholds were assessed over time. n=5-9/group. Data represent the mean ± SEM. **P<0.01 vs. vehicle-injected mice with DMSO at the corresponding time point. ††P<0.01 vs. PTX-injected mice with DMSO at the corresponding time point.

Figure 12. Activation of REV-ERB prevents GFAP expression in spinal dorsal horn of mice with PSNL. (a) Fourteen days after sciatic nerve injury, either SR9009 (300 nmol) or DMSO was intrathecally injected. Spinal dorsal horn was harvested 3 hours after SR9009 injection. Magnified photomicrographs of the white boxed areas are to the right. Scar bar=100 μm. (b) Quantitative analysis of expression of GFAP in spinal dorsal horn after injection of drugs described above at 3 hours following SR9009 injection. Data indicate mean ratio of sum of GFAP immunofluorescence intensity in

each mice, and expressed as mean ± SEM for six to eight mice. *P<0.05 vs. saline-injected mice with DMSO. †P<0.05 vs. LPS-injected mice with DMSO.

Highlights

1. REV-ERB agonist SR9009 prevented upregulation of pronociceptive molecules in spinal astrocytes.

2. Intrathecal treatment with SR9009 prevented LPS-induced mechanical hypersensitivity.

3. Intrathecal SR9009 treatment prevented LPS-induced GFAP expression in spinal cord.

4. Activation of spinal REV-ERBs ameliorated inflammatory and neuropathic pain.

5. Activation of spinal astrocytic REV-ERBs is crucial in antinociception.

Stimulation of nuclear receptor REV-ERBs suppresses production of pronociceptive molecules in cultured spinal astrocytes and ameliorates mechanical hypersensitivity of inflammatory and neuropathic pain of mice

Norimitsu Morioka[1)], Keitaro Kodama[1)], Mizuki Tomori[1)], Kanade Yoshikawa[1)], Munenori Saeki[1)], Yoki Nakamura[1), 2)], Fang Fang Zhang[1), 3)], Kazue Hisaoka-Nakashima[1)], Yoshihiro Nakata[1)]

1) Department of Pharmacology, Hiroshima University Graduate School of Biomedical & Health Sciences, 1-2-3 Kasumi, Minami-ku, Hiroshima 734-8553, Japan

2) Cellular Pathobiology Section, Integrative Neuroscience Research Branch, National Institute on Drug Abuse IRP, Triad Suite 3305, 333 Cassell Drive, Baltimore, MD 21224

3) Institute of Pharmacology, Taishan Medical University, 619 Changcheng Road, Taian, Shandong 271016, China

Corresponding author; Norimitsu MORIOKA
Address: Kasumi 1-2-3, Minami-ku, Hiroshima 734-8553, Japan
Tel: +81-82-257-5312, Fax: +81-82-257-5314,
e-mail: mnori@hiroshima-u.ac.jp

Number of pages: 46, Number of figures: 10, Number of words: 8505

The authors declare no competing financial interests.

Abstract

The orphan nuclear receptors REV-ERBα and REV-ERBβ (REV-ERBs) are crucial in the regulation of inflammatory-related gene transcription in astroglioma cells, but their role in nociceptive transduction has yet to be elaborated. Spinal dorsal horn astrocytes contribute to the maintenance of chronic pain. Treatment of cultured spinal astrocytes with specific REV-ERBs agonists SR9009 or GSK4112 significantly prevented lipopolysaccharide (LPS)-induced mRNA upregulation of pronociceptive molecules interleukin-1β (IL-1β) mRNA, interleukin-6 (IL-6) mRNA and matrix metalloprotease-9 (MMP-9) mRNA, but not CCL2 mRNA expression. Treatment with SR9009 also blocked tumor necrosis factor-induced IL-1β mRNA, IL-6 mRNA and MMP-9 mRNA. In addition, treatment with SR9009 significantly blocked LPS-induced upregulation of IL-1β protein, IL-6 protein and MMP-9 activity. The inhibitory effects of SR9009 on LPS-induced expression of pronociceptive molecules were blocked by knockdown of REV-ERBs expression with short interference RNA, confirming that SR9009 exerts its effect through REV-ERBs. Intrathecal LPS treatment in male mice induces hind paw mechanical hypersensitivity, and upregulation of IL-1β mRNA, IL-6 mRNA and glial fibrillary acidic protein (GFAP) expression in spinal dorsal horn. Intrathecal pretreatment of SR9009 prevented the onset of LPS-induced mechanical hypersensitivity, cytokine expression and GFAP expression. Intrathecal injection of

SR9009 also ameliorated mechanical hypersensitivity during the maintenance phase of complete Freund's adjuvant-induced inflammatory pain and partial sciatic nerve ligation-, paclitaxel-, and streptozotocin-induced neuropathy in mice. The current findings suggest that spinal astrocytic REV-ERBs could be critical in the regulation of nociceptive transduction through downregulation of pronociceptive molecule expression. Thus, spinal REV-ERBs could be an effective therapeutic target in the treatment of chronic pain.

Keywords

REV-ERBs; chronic pain; astrocyte; spinal dorsal horn; interleukin-1β; interleukin-6; tumor necrosis factor; siRNA

Abbreviations

CFA; complete Freund's adjuvant, DMEM; Dulbecco's modified Eagle's medium, FCS; fetal calf serum, GAPDH; glyceraldehydes-3-phosphate dehydrogenase, HDAC; histone deacetylase, iNOS; inducible nitric oxide synthase, IL-1β; interleukin-1β, IL-6; interleukin-6, LPS; lipopolysaccharide, MMP; matrix metalloproteinase, NF-κB; nuclear factor-κB, PBS; phosphate buffered saline, PSNL; partial sciatic nerve ligation, siRNA; small interference RNA , TNF; tumor necrosis factor,

Introduction

There are an increasing number patients suffering from chronic pain, including neuropathic and inflammatory pain, which is associated with the growing population of elderly people (Ferreira and de Luca, 2017; Gagliese et al., 2017). In addition, for many of these patients, chronic pain is refractory to treatment with commonly used analgesics such as opioids and non-steroidal anti-inflammatory drugs. A number of studies have shown that dysregulation of the expression of a number of pronociceptive factors such as pro-inflammatory cytokines and chemokines in CNS glial cells contribute to the induction and maintenance of chronic pain (Grace et al., 2014; Ji et al., 2016). While antagonists, neutralizing antibodies and synthesis blockers to pronociceptive molecules show varying degrees of efficacy in a range of chronic pain models, the analgesic effects of these reagents alone are not always robust. This suggests that targeting mechanisms that regulate the production of numerous molecules rather than targeting specific molecules may be crucial in alleviating chronic pain.

REV-ERBα and REV-ERBβ (REV-ERBs) are orphan nuclear receptors encoded by NR1D1 and NR1D2, respectively, which are expressed in various cell types (Kojetin and Burris, 2014). It has been demonstrated that REV-ERBs have crucial functions in the regulation of metabolism, inflammation and tumor growth (Sato et al., 2014; Solt et

al., 2012; Sulli et al., 2018). Like other nuclear receptors, REV-ERBs exert a ligand-dependent inhibitory effect on gene transcription of various molecules (Kojetin and Burris, 2014; Yin and Lazar, 2005). Accumulating evidence has shown that REV-ERBs negatively regulate the expression of various proinflammatory molecules such as the cytokine interleukin-6 (IL-6) and the chemokine CCL2, following binding of the synthetic REV-ERB-specific agonists GSK4112 and SR9009 in macrophages (Sato et al., 2014; Sitaula et al., 2015). A previous finding showed mildly increased mechanical nociceptive sensitivity in REV-ERBα knockout mice (Lee et al., 2016). Furthermore, it is possible that REV-ERBs might be a new target as analgesic for osteoarthritis-induced pain (Das et al., 2018). However, the exact function and role of REV-ERBs in nociceptive transduction under chronic pain states has yet to be elaborated.

Over-activation of astrocytes in spinal dorsal horn contributes to the maintenance of chronic pain (Morioka et al., 2015; Zhuang et al., 2005). Production of pronociceptive molecules by spinal astrocytes could lead to persistent nociceptive hypersensitivity (Gao et al., 2009; Mika et al., 2013; Nakagawa and Kaneko, 2010). Intrathecal administration of fluorocitrate, an astrocytic inhibitor, ameliorated nociceptive hypersensitivity in chronic pain models (Shibata et al., 2011; Zhang et al., 2012b). These observations suggest that modulating spinal astrocytic activity, from an abnormal or pathophysiological state back to the normal, physiological state, could be

crucial in reducing or eliminating nociceptive hypersensitivity.

Stimulation of REV-ERBs expressed in C6 astroglioma cells suppressed cytokine tumor necrosis factor (TNF)-induced expression of both CCL2 and matrix metalloprotease-9 (MMP-9) (Morioka et al., 2016b). However, a role for REV-ERBs in regulating spinal astrocytic function and in nociceptive transduction in particular has yet to be elaborated. Thus, the current study examined the effects of synthetic REV-ERBs specific agonists SR9009 and GSK4112 on REV-ERBs expressed on spinal astrocytes. The endotoxin lipopolysaccharide (LPS) elicits robust neuroinflammation in animal models and is widely used to induce inflammatory pain through activation of astrocytes in the CNS (Li et al., 2014; Lu et al., 2015). The current study examined the effect of REV-ERBs specific agonists on LPS-induced expression of pro-nociceptive molecules by spinal astrocytes and the antinociceptive effects of SR9009 on LPS-induced mechanical hypersensitivity and inflammatory and neuropathic pain in mice.

Materials and Methods

Animals

All experiments utilizing animals were conducted in accordance with the “Guidelines for the Care and Use of Laboratory Animals” established by The Japanese Pharmacological Society and Hiroshima University, and procedures were reviewed and approved by the Committee of Research Facilities for Laboratory Animal Science of Hiroshima University.

Pregnant Wistar rats (13 days) were obtained from Japan SLC, Inc. (Shizuoka, Japan) and 1-day old pups of both sexes were obtained from these rats. Male ddy mice, 6 weeks of age (Japan SLC, Inc.) were maintained in a vivarium, room temperature of 22±2℃, with a 12h light/dark cycle (lights on/off at 8:00 AM/8:00 PM), and given access to food and water available *ad libitum* during the experimental period.

Reagents

Lipopolysaccharide was obtained from Sigma Chemical Co. (St. Louis, MO, USA). SR9009, a REV-ERBs agonist (REV-ERBα EC_{50}=0.67 μM, REV-ERBβ EC_{50}=0.8 μM (Solt et al., 2012)), was obtained from Merck Millipore (Darmastadt, Germany). GSK4112 was purchased from Cayman Chemical (Ann Arbor, MI). GSK4112 is a

synthetic REV-ERBs agonist (The 50% effective concentration (EC_{50}) to REV-ERBα is 0.4 μM. The EC_{50} to REV-ERBβ is not known.) (Grant et al., 2010). RGFP966 is a selective histone deacetylase 3 (HDAC3) inhibitor (50% inhibitory concentration (IC_{50})=0.08 μM), and is reported to have no affinity to other types of HDAC (IC_{50}>15 μM). GSK4112, SR9009 and RGFP966 were dissolved in DMSO to a final concentration of 0.1% DMSO. Recombinant rat TNF was obtained from WAKO Pure Chemical Industries (Osaka, Japan). TNF was dissolved in distilled H_2O. Paclitaxel was obtained from Sawai Pharmaceutical Co., Ltd. (Osaka, Japan).

Cell culture

The preparation of cultured spinal astrocytes has been described previously (Morioka et al., 2018). In brief, spinal cords isolated from neonatal Wistar rats were minced, and then incubated with trypsin and DNase Ⅰ. Dissociated cells were suspended in Dulbecco's modified Eagle's medium (DMEM) supplemented with 10% fetal calf serum (FCS) and penicillin/streptomycin (100 units/ml and 100 μg/ml, respectively). Thereafter, cell suspensions were plated in 75cm^2 tissue culture flasks (7.5-10×10^6 cells/flask) precoated with poly-L-lysine (10 μg/ml). Cells were maintained in a 10% CO_2 incubator at 37℃. After 10 days, the flasks containing mixed glial cells were vigorously shaken and washed with PBS to remove microglial cells.

Remaining cells were trypsinized, and seeded to new flasks. After confluent state, cells were treated with 1 μM of cytosine β-D-arabinofuranoside (Sigma) to prevent proliferation of other cells such as microglia and fibroblasts for 2 days. Then, the flasks were again vigorously shaken and washed, and the cells were trypsinized. Thereafter, the remaining cells were transferred to 35-mm dishes (3-3.5×10^5 cells). After 3 days, the medium was replaced with DMEM without FCS and antibiotics. After an additional 24 hours of incubation, the cells were used in experiments. Greater than 95% of the cells obtained using the current method expressed an astrocytic phenotype as confirmed by RT-PCR and Western blotting (Morioka et al., 2014).

Rat cultured spinal astrocytes have been shown to express Rev-erbα mRNA and Rev-erbβ mRNA (Morioka et al., 2016b). To induce expression of pro-nociceptive molecules, cells were incubated with either LPS (10 ng/ml) or TNF (10 ng/ml). The role of REV-ERBs in LPS-induced gene expression was assessed using pharmacological agents. Compounds that activated REV-ERB were incubated in astrocytes for 30 min followed by LPS or TNF incubation for up to 24 hours. Cell medium and cells were removed for assay at specific time points during LPS or TNF incubation (see Results).

Real-time PCR analysis

cDNA synthesized using 1 μg of total RNA from cultured spinal astrocytes and mice spinal tissue were subjected to real-time PCR assay with specific primers and EXPRESS SYBR® GreenER™ qPCR SuperMix (Invitrogen, Carlsbad, CA, USA). The sequences of the primers are described in previous reports (Morioka et al., 2018; Zhang et al., 2016). Real-time PCR assays were conducted using a DNA engine Opticon 2 real-time PCR detection system (Bio-Rad, Hercules, CA, USA). The three-step amplification protocol consisted of 3 min at 95℃ followed by 40 cycles of 95℃ for 15 s, 60℃ for 30 s, and 72℃ for 30 s. RNA quantification of target genes was calculated using the C_t method. The C_t values of each amplification were normalized to those obtained with the amplification of glyceraldehydes-3-phosphate dehydrogenase (GAPDH).

Transfection of primary cultured astrocytes with small interfering RNA (siRNA)

Forty-eight hours after the cells were seeded, the culture was replaced with Opti-MEM medium (Invitrogen, Carlsbad, CA, USA), and then the cells were transfected with either siRNA, targeting rat *Rev-erbα* (siGENOME SMARTpool, Rat Nr1d1, GE Dharmacon, Lafayette, CO, USA), *Rev-erbβ* (siGENOME SMARTpool, Rat Nr1d2, GE Dharmacon) or non-targeting siRNA (siGENOME Non-Targeting siRNA Pool #2) by using Lipofectamine RNAi MAX reagent (Invitrogen). Twenty-four hours after

transfection, cells were treated with SR9009 for 30 min. Then, cells were further treated with LPS for 24 hours.

ELISA

Rat IL-1β, IL-6 and CCL2 protein levels in cell-conditioned medium were measured using ELISA kits (eBioscience, San Diego, CA, USA). After treatment with SR9009 for 30 min, astrocytes were stimulated with LPS for 24 hours. Then, culture media were immediately collected and stored at -80℃ until assay. Each reaction was performed according to the manufacturer's protocol.

Gelatin zymography

To measure the activity of MMP-9, a gelatinase, gelatin zymography was performed based on methods described previously (Abe et al., 2016). In brief, after drug treatment, the culture supernatant of primary astrocytes was collected, and the supernatant was added to sample buffer (125 mM Tris-HCl, pH 6.8, 1% glycerol, 2% SDS, 0.01% bromophenol blue), and equal amount of protein were separated by electrophoresis using 8% SDS-polyacrylamide gel containing 0.1% gelatin under non-reducing condition. After separation, gels were incubated with 2.5% Triton X-100 for 1 hour, and further incubated with the buffer (50 mM Tris-HCl (pH 7.4, 10 mM $CaCl_2$,

0.02% NaN_3) for 20 hours at 37℃. Then, gels were incubated with the staining solution (0.125% Coomassie Brilliant Blue R-250, 30% ethanol, 10% acetic acid) for 3 hours, and destained in 25% methanol/7.5% acetic acid until bands showing gelatinolysis are clearly appeared. The density of specific band for MMP-9 was identified dependent on the molecular size (83 kDa) of MMP-9 described previous study (Abe et al., 2016) and using by the MMP Marker (PMC Cosmobio, Tokyo, Japan). The density was measured with Science Lab Image Gauge (Fuji Film, Tokyo, Japan).

Mouse intrathecal injection

Intrathecal injections were performed on unanesthetized mice. In brief, mice were restrained with the left hand and the injection was performed with the right hand. The vertebral landmarks for L5 and L6 vertebrate were identified by palpation. An injection into the subarachnoid space between the L5 and the L6 vertebrae was done via a 27-gage needle. Entry of the needle was confirmed with the presence of a tail flick. The injection volume of all other compounds was 5 μl.

Inflammatory pain models

Inflammation was induced by either intrathecal injection of LPS (0.1 μg/5 μl saline) or

subcutaneous injection of complete Freund's adjuvant (CFA; 30 μl, 1mg of Mycobacterium tuberculosis/ml, Sigma) into the center of the plantar surface of left hind-paw in mice. The same volume of saline was used as a control.

Partial sciatic nerve ligation (PSNL)-induced neuropathic pain model

Under sodium pentobarbital (50 mg/kg, i.p.) anesthesia, a tight ligation of approximately one-third to one-half of the diameter of the left sciatic nerve (ipsilateral) was performed with 8-0 silk suture as described previously (Morioka et al., 2016a). In sham-operated mice, the sciatic nerve was exposed but not ligation. Previous studies have demonstrated that mechanical hypersensitivity was observed 3 days, and lasted at 3 weeks following PSNL (Morioka et al., 2015; Nakamura et al., 2015).

Paclitaxel-induced neuropathic pain model

Paclitaxel was dissolved in cremophor:ethanol (1:1) as the stock solution (6 mg/ml). This was diluted in saline to a final concentration of 0.2 mg/ml. The vehicle for paclitaxel was diluted with saline at the same proportion as the paclitaxel solution. Then, paclitaxel (2 mg/kg) was intraperitoneally administered in a volume of 0.1 mL/20 g once per day for 5 times every other day (cumulative dose 10 mg/kg).

Diabetes-induced neuropathic pain model

Diabetes was induced in mice fasted overnight by an injection of streptozotocin (Cayman Chemical). Streptozotocin was dissolved in saline immediately before injection and the solution administered intraperitoneally at a dose of 200 mg/kg. Control animals received a vehicle injection. Blood samples were collected from tail vein, and blood glucose levels were measured by a glucometer (Freestyle Freedom Lite; NIPRO, Osaka, Japan). Hyperglycemic mice (>300 mg/dl) at 21 days after streptozotocin injection were used for further analysis.

Hind paw sensitivity to mechanical stimulation

All behavioral assessments were performed blinded. The withdrawal threshold (in grams) of the hind paw to mechanical stimulation was determined using von Frey filaments (Morioka et al., 2015). In brief, a von Frey filament was pressed against the mid-planter surface of the hind paw. The lowest force that caused responses such as lifting and licking of the hind paw was assigned as the withdrawal threshold. Each hind paw was tested three times, at 10 second intervals, and the mean withdrawal threshold was reported. Mice with inflammation, PSNL or paclitaxel that did not show robust mechanical hypersensitivity, hind paw withdrawal threshold >0.1 g, were excluded from the experiments. Prior to treatment, hind paw withdrawal thresholds

were 1.0±0.2 g (mean±SEM).

In LPS-treated mice, either 100 or 300 nmol of SR9009 or 100 nmol of GSK4112 were intrathecally treated 1 hour before LPS injection. Withdrawal thresholds were measured 1, 2, 3, 6 and 24 hours following the second intrathecal injection. In CFA-treated mice, 7 days following intraplantar treatment of CFA, mice received either an intrathecal treatment of 100 or 300 nmol of SR9009 or 100 nmol of GSK4112. Withdrawal thresholds were then measured 1, 2, 3, 6 and 24 hours post-injection. In PSNL mice, 14 days following surgery, mice received an intrathecal treatment of 100 or 300 nmol of SR9009. Withdrawal thresholds were then measured 1, 2, 3, 4, 5 and 24 hours post-injection. In paclitaxel mice, 14 days following the injection (6 days following the last injection), mice received an intrathecal treatment of 100 or 300 nmol of SR9009. Withdrawal thresholds were then measured 1, 2, 3, 6 and 24 hours post-injection. In diabetic mice, 21 days following the injection of streptozotocin, mice received an intrathecal treatment of 100 or 300 nmol of SR9009. Withdrawal thresholds were then measured 1, 2, 3, 6 and 24 hours post-injection.

Immunohistochemistry

Tissue sections of spinal dorsal horn from at least 3 mice of each treatment were used for immunohistochemistry. Thirty minutes after intrathecal administration of

SR9009, mice were further intrathecally injected of LPS. Fourteen days following PSNL, SR9009 was intrathecally injected. Then, after 3 hours, mice were anesthetized with isoflurane (induction; 5%, maintenance; 2-3%) and sodium pentobarbital (50 mg/kg, i.p.). Mice were transcardially perfused with 50 ml of saline followed by 100 ml of freshly prepared 4% (w/v) paraformaldehyde in 0.1 M phosphate buffer (pH = 7.4). The spinal tissues were quickly removed and postfixed in 4% paraformaldehyde in 0.1 M phosphate buffer for three days at 4°C and then cryoprotected overnight in 30% (w/v) sucrose in 0.1 M phosphate buffer at 4°C. Tissues were embedded in Tissue-Tek OCT compound 4583 (Sakura Finetech, Tokyo, Japan) and frozen in liquid nitrogen, cut serially (20 μm thickness) in a cryostat, and collected onto glass slides. After slides were dried at room temperature, tissue sections were processed for double-labeling immunohistochemistry. Tissue sections were rinsed with phosphate-buffered saline, incubated in a blocking solution of 10% goat serum, 3% bovine serum albumin, 0.1% Triton X and 0.05% Tween-20 in phosphate-buffered saline for 2 hours at room temperature, and then incubated with rabbit anti-glial fibrillary acidic protein (GFAP) antibody (1:1,000, GTX72747, GeneTex Inc., Irvine, CA, USA). Tissues were incubated in primary antibodies for 72 hours at 4°C, followed by corresponding secondary antibodies conjugated with Alexa Fluor® 488 (1:500) for 2 hours at 4°C in a dark chamber. The sections were then

extensively washed in phosphate-buffered saline and coverslipped. Sections were examined with a BZ-9000 Biorevo all-in-one fluorescence microscope (Keyence, Elmwood Park, NJ, USA).

Statistical analysis

Data are expressed as the mean±SEM of at least three independent determinations. The effects of drug treatment on mRNA and protein levels were performed using a one-way analysis of variance (ANOVA) with a pairwise comparison by the Tukey-Kramer method. Comparisons between two groups were performed using Student's t-test. Possible interactions between treatment over time on mechanical hypersensitivity were analyzed by two-way repeated-measures ANOVA, followed by the Tukey-Kramer method for post hoc comparisons. Differences were considered to be significant when the P value was less than 0.05.

Results

REV-ERBs agonists block LPS-induced production of pronociceptive molecules in cultured spinal astrocytes

Treatment of cultured spinal astrocytes with LPS markedly upregulated mRNA expression of pro-nociceptive molecules, including IL-1β, IL-6, MMP-9 and CCL2 (Fig. 1a-1d). Induction of IL-β mRNA expression was observed 1 hour, peaked 6 hours and declined 24 hours after treatment with LPS (Fig. 1a). The inhibitory effect of a specific REV-ERBs agonist SR9009 on LPS-induced IL-β mRNA expression was observed beginning 1 hour after treatment with LPS, and this effect lasted over the 24 hours incubation period (Fig. 1a). Although LPS-induced IL-6 mRNA expression was also observed 1 hour after LPS incubation, induction of IL-6 mRNA was significantly prevented by pretreatment with SR9009 at 6 and 24 hours (Fig. 1b). MMP-9 mRNA expression was significantly induced 3 hours after LPS treatment, and inhibitory effect of SR9009 on the MMP-9 mRNA expression was also observed at the same time and this effect lasted 24 hours (Fig. 1c). Induction of CCL2 mRNA was observed 1 hour after LPS treatment--SR9009 had no effect on LPS-induced CCL2 mRNA expression (Fig. 1d). Incubation of cultured spinal astrocytes with 10 μM of SR9009 alone did not significantly affect mRNA expression of pronociceptive molecules (Fig. 1). Pretreatment with SR9009 (3, 5 and 10 μM) significantly suppressed the stimulatory

effects of LPS on IL-1β mRNA, IL-6 mRNA and MMP-9 mRNA in a concentration-dependent manner (Fig. 2a-2c). Although SR9009 slightly inhibited LPS-induced CCL2 mRNA expression, this effect was not statistically significant (Fig. 2d). Furthermore, pretreatment with 10 and 20 μM of GSK4112, also a REV-ERB agonist, significantly suppressed LPS-induced mRNA expression of IL-1β, IL-6, MMP-9, but not CCL2 (Fig. 3a-3d). Incubation of cultured spinal astrocytes with 20 μM of GSK4112 alone did not significantly affect mRNA expression of pronociceptive molecules (Fig. 3). In addition, pretreatment with SR9009 also significantly blocked TNF-induced mRNA expression of IL-1β, IL-6 and MMP-9 (Fig. 4a-4c). In TNF-treated cells, similar to that observed following LPS treatment, SR9009 showed a trend towards inhibition of CCL2 mRNA expression, which was not statistically significant (Fig. 4d).

SR9009 inhibited LPS-induced protein expression of IL-1β, IL-6, CCL2 and MMP-9. Treatment with SR9009 (10 μM) significantly inhibited LPS-induced production of IL-1β, IL-6, but not CCL2 (Fig. 5a-5c). Furthermore, gelatin zymography showed that stimulation with LPS increased the activity of MMP-9 released into the cultured medium, and this effect was significantly blocked by pretreatment with SR9009 (Fig. 5d). Incubation of cultured spinal astrocytes with 10 μM of SR9009 alone did not significantly affect protein expression of pronociceptive molecules (Fig. 5a-5d).

As mentioned earlier, cultured spinal astrocytes express both Rev-erbα mRNA and Rev-erbβ mRNA (Morioka et al., 2016b), and SR9009 acts on both types of REV-ERBs with almost equal affinity (Solt et al., 2012). Thus, siRNA was used to inhibit expression of Rev-erbα mRNA and Rev-erbβ. As shown in Fig. 6a, the expression of both Rev-erbα mRNA and Rev-erbβ mRNA in cultured spinal astrocytes was significantly reduced after 48 hours of incubation with both siRNAs. Although significant inhibition by SR9009 on LPS-induced expression of IL-1β mRNA and MMP-9 mRNA was observed following knockdown of both Rev-erbs, the inhibitory effects of SR9009 were significantly reduced (Fig. 6b, 6d). Significant knockdown of both Rev-erbs mRNA almost completely reversed inhibitory effect of SR9009 on LPS-induced IL-6 mRNA expression (Fig. 6c). Thus, these results demonstrate that stimulation of REV-ERBs prevent the expression of pro-nociceptive molecules in spinal astrocytes.

Histone deacetylase 3 is a crucial mediator of the inhibitory effects of REV-ERBs on LPS-induced mRNA upregulation of IL-1β and IL-6, but not MMP-9, in cultured spinal astrocytes

Previous studies have demonstrated that REV-ERBs repress gene transcription through recruitment of nuclear receptor corepressor 1 (NCoR1) and HDAC3. Thus,

astrocytes were pretreated with the HDAC3 inhibitor RGFP966. RGFP966 (2 μM) reversed the inhibitory effect of SR9009 on LPS-induced expression of IL-1β mRNA and IL-6 mRNA (Fig. 7a, 7b). However, pretreatment with RGFP966 did not reverse LPS-induced expression of MMP-9 mRNA (Fig. 7c). Treatment with RGFP966 alone, without LPS and SR9009, did not affect IL-1β, IL-6 and MMP-9 mRNA expression. These results indicate that HDAC3 is necessary in the inhibitory effect of REV-ERBs on inducing IL-1β and IL-6 transcription with LPS. However, in the case of LPS-induced MMP-9 transcription, molecular mechanisms other than HDAC3 could be involved in the inhibitory effect of REV-ERB.

Stimulation of spinal REV-ERBs with specific agonists prevents LPS-induced mechanical hypersensitivity through downregulation of pronociceptive molecules

Potential antinociceptive effects of the activation of spinal REV-ERBs on LPS-induced hind paw mechanical hypersensitivity were examined. Intrathecal treatment with LPS induced significant mechanical hypersensitivity beginning 1 hour after injection, and lasted for as long as 24 hours after injection (Fig. 8). Intrathecal pretreatment with either SR9009 (100 and 300 nmol) or GSK4112 (100 nmol) prevented the onset of LPS-induced mechanical hypersensitivity (Fig. 7a; LPS versus

LPS+SR9009 100 nmol; $F_{1,144}$=15.3, P<0.001, interaction effect, $F_{1,144}$=3.36, P=0.00669, LPS versus LPS+SR9009 300 nmol; $F_{1,159}$=47.4, P<0.001, interaction effect, $F_{1,159}$=6.00, P<0.001, LPS versus LPS+GSK4112 100 nmol; $F_{1,127}$=14.5, P<0.001, interaction effect, $F_{1,127}$=5.17, P<0.001). Treatment with SR9009 alone had no effect on withdrawal thresholds of saline-treated mice (Fig. 8).

The effect of SR9009 on the expression of IL-1β, IL-6 and MMP-9 in spinal dorsal horn of mice following intrathecal treatment with LPS was examined. As the current study showed that antinociception with SR9009 was at least observed between 2-6 hours following administration of LPS, the effect of SR9009 on pronociceptive molecules expression was examined 3 hours after intrathecal treatment with LPS. The expression of both IL-1β and IL-6 mRNA was significantly increased in spinal dorsal horn following LPS treatment (Fig. 9a and 9b). Intrathecal pretreatment with SR9009 (100 and 300 nmol) significantly reduced both IL-1β and IL-6 mRNA expression in mice spinal dorsal horn treated with LPS (Fig. 9a and 9b). Intrathecal pretreatment with SR9009 alone did not change either IL-1β or IL-6 mRNA expression (Fig. 9a and 9b). In contrast to in vitro findings, intrathecal treatment with LPS did not significantly induce MMP-9 mRNA expression. Intrathecal SR9009 treatment in mice either with or without intrathecal LPS treatment did not affect MMP-9 mRNA expression (Fig. 9c).

Intrathecal treatment with SR9009 prevents LPS-induced GFAP expression in spinal dorsal horn

An increase of GFAP immunoreactivity, a cellular marker for astrocytes, was observed in the spinal dorsal horn 3 hours following intrathecal injection of LPS, indicating the presence of activated astrocytes. Intrathecal saline injection did not change GFAP expression. Mice were intrathecally pretreated with SR9009 (300 nmol) and 30 min later were intrathecally injected with LPS. SR9009 prevented LPS-induced GFAP expression in spinal dorsal horn (Fig. 10). The findings suggest that activation of REV-ERBs prevents astrocytic activation.

Effect of SR9009 on mechanical hypersensitivity in mouse models of inflammatory and neuropathic pain

The effect of SR9009 on CFA-induced peripheral inflammatory pain was investigated (Fig. 11a). After 7 days, intraplantar injection of CFA significantly decreased withdrawal thresholds to mechanical stimuli, indicating mechanical hypersensitivity (Fig. 11a). Intrathecal treatment with SR9009 (300 nmol) significantly ameliorated CFA-induced mechanical hypersensitivity (CFA versus CFA+SR9009 300 nmol; $F_{1,108}$=34.2, P<0.001, interaction effect, $F_{1,108}$=4.03, P=0.00215). Antinociceptive effect of SR9009 was observed beginning 2 hours after injection, and sustained for at

least 3 hours after injection (Fig. 11a). Treatment of saline-treated mice with SR9009 had no effect on withdrawal thresholds (Fig. 11a).

A potential antinociceptive effect of SR9009 on various types of neuropathic pain (PSNL, paclitaxel and streptozotocin) was examined. Fourteen days after surgery, intrathecal injection of SR9009 significantly reversed mechanical hypersensitivity in a dose-dependent manner in PSNL mice (Fig. 11b; PSNL versus PSNL+SR9009 100 nmol; $F_{1,155}$=42.5, P<0.001, interaction effect, $F_{1,155}$=12.0, P<0.001, PSNL versus PSNL+SR9009 300 nmol; $F_{1,151}$=74.3, P<0.001, interaction effect, $F_{1,151}$=14.1, P<0.001). The antinociceptive effect of 300 nmol SR9009 was observed beginning 2 hours after injection and sustained for at least 3 hours after injection. Intrathecal injection of SR9009 (100 nmol) also significantly increased withdrawal thresholds to mechanical stimuli for about 3 hours after injection in PSNL mice (Fig. 11b). Intrathecal treatment with SR9009 (300 nmol) in sham-operated mice had no effect on withdrawal thresholds (Fig. 11b).

Significant mechanical hypersensitivity was observed 14 days following the first injection of paclitaxel (Fig. 11c). Intrathecal treatment with SR9009 significantly ameliorated paclitaxel-induced mechanical hypersensitivity (Fig. 11c; paclitaxel versus paclitaxel+SR9009 100 nmol; $F_{1,72}$=117.94, P<0.001, interaction effect, $F_{1,72}$=9.00, P<0.001). The antinociceptive effect of 100 nmol SR9009 was significant

beginning 1 hour after injection and lasted for at least 6 hours after injection (Fig. 11c). By contrast, the antinociceptive effect of 300 nmol SR9009 was observed 2 hours after injection (Fig. 11c). Intrathecal injection of SR9009 (300 nmol) in vehicle-treated mice had no effect on withdrawal thresholds (Fig. 11c).

Significant mechanical hypersensitivity was observed three weeks following the injection of streptozotocin (Fig. 11d). Intrathecal treatment with 300 nmol of SR9009 significantly ameliorated streptozotocin-induced mechanical hypersensitivity (Fig. 11d; streptozotocin versus streptozotocin+SR9009 300 nmol; $F_{1,66}$=82.9, P<0.001, interaction effect, $F_{1,66}$=22.2, P<0.001). The antinociceptive effect of 300 nmol SR9009 was observed beginning 2 hours after injection, and lasted for at least 3 hours after injection (Fig. 11d). By contrast, no antinociceptive effect was observed with 100 nmol SR9009 (Fig. 11d). Intrathecal injection of SR9009 (300 nmol) in vehicle-treated mice had no effect on withdrawal thresholds (Fig. 11d).

Intrathecal treatment with SR9009 reverses upregulation of GFAP in spinal dorsal horn following sciatic nerve injury

Fourteen days following PSNL, during the period of significant mechanical hypersensitivity, spinal dorsal horn GFAP expression was significantly increased compared than that of sham mice (Fig. 12a and 12b). Treatment with SR9009 (300

nmol) significantly suppressed PSNL-induced GFAP expression in spinal dorsal horn (Fig. 12a and 12b). Treatment with vehicle or SR9009 alone had no effect on GFAP expression in spinal dorsal horn of sham mice (Fig. 12a and 12b).

Discussion

The current study examined whether REV-ERBs could be targeted to relieve pain in various chronic pain states. In the current study, activation of cultured spinal astrocytes' REV-ERBs prevented the expression of pronociceptive molecules by an inflammatory stimulus. During the maintenance phase of chronic pain, pronociceptive molecules produced by activated spinal astrocytes have a crucial role in mediating nociceptive hypersensitivity. In mice, activation of spinal REV-ERBs prevented LPS-induced mechanical hypersensitivity through the downregulation of IL-1β and IL-6 expression in spinal dorsal horn. Furthermore, activation of spinal REV-ERBs in mice reversed inflammatory and neuropathic mechanical hypersensitivity. In addition, stimulation of spinal REV-ERBs blocked upregulation of astrocytic activation marker protein GFAP in spinal dorsal horn of inflammatory and neuropathic pain model mice. Thus, the current findings suggest that astrocytic REV-ERBs could be crucial in the regulation of nociceptive transduction through the inhibition of the production of pronociceptive molecules.

Significant involvement of REV-ERBs in the regulation of the response to inflammatory stimulation has been previously reported. Activation of REV-ERBs suppressed TNF-induced expression of CCL2 mRNA and MMP-9 mRNA, but not IL-6 mRNA and inducible nitric oxide synthase mRNA, in C6 glioma cells (Morioka et al.,

2016b). REV-ERBs appear to modulate the expression of proinflammatory molecules of various immune cells. Co-treatment with SR9009 blocked LPS and interferon-γ-induced expression of IL-6 mRNA and IL-1β mRNA in mouse bone marrow-derived macrophages and activation REV-ERBα blocked IL-6 and CCL2 expression in mouse peritoneal macrophage (Sato et al., 2014; Sitaula et al., 2015). Mutation of REV-ERBs in bronchial epithelia augmented inflammatory responses and chemokine production, demonstrating the importance of activated REV-ERBs in the response to inflammatory stimuli (Pariollaud et al., 2018). Although *Rev-erb* mRNA expression has been observed in cultured spinal astrocytes (Morioka et al., 2016b), there are no reports regarding the function of REV-ERB subtypes in spinal astrocytes.

The current study demonstrated that activation of REV-ERBs expressed on cultured spinal astrocytes suppressed LPS-induced expression of IL-1β, IL-6 and MMP-9. The proinflammatory cytokine TNF, which is mainly produced from activated microglia, has been shown to induce the production of pronociceptive molecules and evoke mechanical hypersensitivity, possibly through the activation of spinal astrocytes (Grace et al., 2014; Morioka et al., 2014). In the current study, activation of spinal astrocytic REV-ERBs also prevented TNF-induced expression of IL-1β, IL-6 and MMP-9. Thus, it is possible that REV-ERBs could suppress activation of astrocytes regardless of the inflammatory stimulus. REV-ERBs activation partially inhibited

induction of CCL2 expression, indicating that REV-ERBs play a minor role in the expression of this pronociceptive molecule and further suggests that REV-ERBs modulate the expression of many but not all pronociceptive molecules. The inhibitory effects of REV-ERBs agonist SR9009 can be attributed to direct stimulation of REV-ERBs, as knockdown of both subtypes of REV-ERB by RNA interference led to a lack of efficacy of the agonist and SR9009 has no significant cross-activity against other members of the nuclear receptor superfamily (Solt et al., 2012). Together, these findings indicate that activation of spinal astrocytic REV-ERBs have a significant role in mediating antinociception.

REV-ERBs bind to retinoic acid receptor-related orphan receptors (RORs) element (RORE) and compete in binding of positive transcriptional factor RORs (Kojetin and Burris, 2014; Sato et al., 2014). Furthermore, it has been shown that the HDAC3-dependent transcriptional inhibition by REV-ERB activation could be mediated through the modulation of response elements different from that of the RORE motif (Zhang et al., 2015). These are the potential mechanism mediating REV-ERBs inhibition of transcription. The current study showed that HDAC3 activity is crucial in the inhibitory effects of REV-ERBs on LPS-induced expression of IL-1β and IL-6, but not MMP-9. Thus, it is possible that the effect of REV-ERBs on MMP-9 in spinal astrocytes could be regulated by a RORs-dependent mechanism. By contrast, a

previous study demonstrated that the inhibitory effect of REV-ERBs on MMP-9 induction is dependent on HDAC3 in C6 glioma cells (Morioka et al., 2016b). Thus, these findings suggest that a REV-ERBs-mediated inhibitory mechanism could be dependent whether a ROR element or HDAC3-acting sites exist in the promoter regions of the target gene in different cell types.

Activated spinal astrocytes have a key role in the maintenance of nociceptive hypersensitivity during the chronic pain state, so targeting astrocytic activity could lead to significant analgesia. While there are a number of mechanistic distinctions between inflammatory and neuropathic pain, it has been found that activation of spinal astrocytes is crucial across these models (Deng et al., 2017; Morioka et al., 2015; Qian et al., 2016). In the case of paclitaxel-induced neuropathy and PSNL, mechanical hypersensitivity appears to be mainly mediated through activation of spinal dorsal horn astrocytes and not microglia (Li et al., 2014; Morioka et al., 2015; Zhang et al., 2012a). Intrathecal LPS-induced mechanical hypersensitivity is likely due to activation of astrocytes in spinal dorsal horn (Lu et al., 2015; Saito et al., 2010; Zhao et al., 2014) and in the current study activation of REV-ERBs reduced both LPS- and PSNL-induced GFAP expression in spinal dorsal horn as well as suppressed mechanical hypersensitivity in both pain model mice. It is possible, then, that the antinociceptive effect of REV-ERBs activation observed across the current set of

chronic pain models could be mediated, in part, by suppression of astrocytic activation.

While astrocytic functional status, such as GFAP immunoreactivity, was not directly assessed in the neuropathic and inflammatory pain models in the current study, reduced astrocytic functioning following REV-ERBs activation was inferred by reduced production of pronociceptive cytokines (Grace et al., 2014; Hansen and Malcangio, 2013; Nakagawa and Kaneko, 2010). The current study confirmed previous finding, in that stimulation of spinal dorsal horn astrocytes in vivo with LPS upregulated pronociceptive molecules, including IL-1β and IL-6, (Lu et al., 2015; Zhao et al., 2014). Previous studies also showed that these molecules mediate LPS-induced hypersensitivity (Loram et al., 2011; Zhu et al., 2014). In the current study, upregulation of IL-1β and IL-6 was prevented and mechanical hypersensitivity was reduced with intrathecal treatment with a REV-ERB agonist. Thus, the decreased expression of pronociceptive molecules and decreased mechanical hypersensitivity observed following spinal REV-ERBs activation suggests decreased spinal astrocytic activation.

The inhibitory role of REV-ERBα in gene expression is well known. REV-ERBβ contributes to the regulation of genes involved in lipid and energy homeostasis in skeletal muscle cells (Ramakrishnan et al., 2005). Furthermore, several types of

tumor cell predominantly express REV-ERBβ, and genetic or pharmacological inhibition of REV-ERBβ sensitizes cancer cells to the cytotoxic reagent chloroquine, which suppresses autophagy (De Mei et al., 2015). In the current study, the inhibitory role of each REV-ERB on the expression of pronociceptive molecules was not clearly demarcated. Preliminary findings suggested that although knockdown of both REV-ERBs by RNA interference prevented SR9009-induced suppression of gene expression in cultured spinal astrocytes, knockdown of either REV-ERB alone did not (data not shown). Thus, each REV-ERB subtype could have a distinct function in regulating IL-6, IL-1β and MMP-9 transcription in spinal astrocytes.

A number of studies demonstrated that activation of REV-ERBs suppresses MMP-9 expression in various cell types (Lam et al., 2013; Morioka et al., 2016b; Song et al., 2018; Stujanna et al., 2017). Interestingly, in the current study, while in vitro astrocytic expression of MMP-9 mRNA increased following LPS treatment, spinal dorsal horn MMP-9 expression was not changed following intrathecal LPS treatment. Therefore, it is possible that MMP-9 might not be involved in LPS-induced nociceptive hypersensitivity in vivo. Alternatively, it is possible that MMP-9 is involved in late-stage maintenance of LPS-induced hypersensitivity, as the current study found peak in vitro expression of MMP-9 mRNA was later than that of IL-1β mRNA and IL-6 mRNA. In vivo findings in inflammatory and neuropathic pain models suggest that spinal MMP-9

is likely involved in late-stage maintenance of pain (Jiang et al., 2017; Kular et al., 2012). Although further investigation is needed, downregulation of MMP-9 could be one of the mechanisms underlying the antinociceptive effect of SR9009 and MMP-9 could be an important molecule mediating established nociceptive hypersensitivity across a variety of pain states.

While the current study confirms a role of spinal astrocytes in the maintenance of chronic pain, activated spinal microglial REV-ERBs could also have an antinociceptive function. Intrathecal injection of LPS activates both spinal dorsal horn microglia and astrocytes (Saito et al., 2010; Zhao et al., 2014; Zhu et al., 2014). Treatment of cultured mouse brain microglia with the REV-ERB agonist SR9011 suppressed LPS-induced IL-6 expression (Nakazato et al., 2017). Therefore, it is possible that spinal microglial REV-ERBs could modulate spinal IL-1β and IL-6 mRNA expression in the current study, thereby contributing to REV-ERB agonist-mediated antinociception observed in the current study. However, whether spinal microglial REV-ERBs regulate the expression of proinflammatory molecules is not unknown.

In conclusion, the current findings demonstrated that stimulation of spinal astrocytic REV-ERBs suppressed astrocytic functioning, as inferred by decreased production of pronociceptive molecules IL-1β and IL-6. Stimulation of spinal astrocytic REV-ERBs could be effective in a wide range of pain states as astrocytes have a key role in

mediating chronic pain, regardless of etiology. Therefore, targeting spinal astrocytic REV-ERBs could be a novel therapeutic strategy for ameliorating chronic pain.

Acknowledgements

This work was supported by Grant-in-Aid for Scientific Research (C) grant number 26460342, and grants from the Takeda Science Foundation, Suzuken Memorial Foundation, The Uehara Memorial Foundation and The Nakatomi Foundation. Experiments were carried out using equipment at the Analysis Center of Life Science, Hiroshima University and the Research Center for Molecular Medicine, Faculty of Medicine, Hiroshima University. We also thank Dr. Aldric T. Hama for his critical reading of the manuscript.

References

Abe, H., Hisaoka-Nakashima, K., Kajitani, N., Okada-Tsuchioka, M., Yano, R., Itagaki, K., Shibasaki, C., Morioka, N., Nakata, Y., Takebayashi, M., 2016. The expression of glial cell line-derived neurotrophic factor mRNA by antidepressants involves matrix metalloproteinase-9 activation in rat astroglial cells. Biochem Biophys Res Commun 479, 907-912.

Das, V., Kc, R., Li, X., Varma, D., Qiu, S., Kroin, J.S., Forsyth, C.B., Keshavarzian, A., van Wijnen, A.J., Park, T.J., Stein, G.S., O-Sullivan, I., Burris, T.P., Im, H.J., 2018. Pharmacological targeting of the mammalian clock reveals a novel analgesic for osteoarthritis-induced pain. Gene 655, 1-12.

De Mei, C., Ercolani, L., Parodi, C., Veronesi, M., Lo Vecchio, C., Bottegoni, G., Torrente, E., Scarpelli, R., Marotta, R., Ruffili, R., Mattioli, M., Reggiani, A., Wade, M., Grimaldi, B., 2015. Dual inhibition of REV-ERBβ and autophagy as a novel pharmacological approach to induce cytotoxicity in cancer cells. Oncogene 34, 2597-2608.

Deng, X.T., Wu, M.Z., Xu, N., Ma, P.C., Song, X.J., 2017. Activation of ephrinB-EphB receptor signalling in rat spinal cord contributes to maintenance of diabetic neuropathic pain. Eur J Pain 21, 278-288.

Ferreira, M.L., de Luca, K., 2017. Spinal pain and its impact on older people. Best Pract Res Clin Rheumatol 31, 192-202.

Gagliese, L., Gauthier, L.R., Narain, N., Freedman, T., 2017. Pain, aging and dementia: Towards a biopsychosocial model. Prog Neuropsychopharmacol Biol Psychiatry.

Gao, Y.J., Zhang, L., Samad, O.A., Suter, M.R., Yasuhiko, K., Xu, Z.Z., Park, J.Y., Lind, A.L., Ma, Q., Ji, R.R., 2009. JNK-induced MCP-1 production in spinal cord

astrocytes contributes to central sensitization and neuropathic pain. J Neurosci 29, 4096-4108.

Grace, P.M., Hutchinson, M.R., Maier, S.F., Watkins, L.R., 2014. Pathological pain and the neuroimmune interface. Nat Rev Immunol 14, 217-231.

Grant, D., Yin, L., Collins, J.L., Parks, D.J., Orband-Miller, L.A., Wisely, G.B., Joshi, S., Lazar, M.A., Willson, T.M., Zuercher, W.J., 2010. GSK4112, a small molecule chemical probe for the cell biology of the nuclear heme receptor Rev-erbα. ACS Chem Biol 5, 925-932.

Hansen, R.R., Malcangio, M., 2013. Astrocytes--multitaskers in chronic pain. Eur J Pharmacol 716, 120-128.

Ji, R.R., Chamessian, A., Zhang, Y.Q., 2016. Pain regulation by non-neuronal cells and inflammation. Science 354, 572-577.

Jiang, L., Pan, C.L., Wang, C.Y., Liu, B.Q., Han, Y., Hu, L., Liu, L., Yang, Y., Qu, J.W., Liu, W.T., 2017. Selective suppression of the JNK-MMP2/9 signal pathway by tetramethylpyrazine attenuates neuropathic pain in rats. J Neuroinflammation 14, 174.

Kojetin, D.J., Burris, T.P., 2014. REV-ERB and ROR nuclear receptors as drug targets. Nat Rev Drug Discov 13, 197-216.

Kular, L., Rivat, C., Lelongt, B., Calmel, C., Laurent, M., Pohl, M., Kitabgi, P., Melik-Parsadaniantz, S., Martinerie, C., 2012. NOV/CCN3 attenuates inflammatory pain through regulation of matrix metalloproteinases-2 and -9. J Neuroinflammation 9, 36.

Lam, M.T., Cho, H., Lesch, H.P., Gosselin, D., Heinz, S., Tanaka-Oishi, Y., Benner, C., Kaikkonen, M.U., Kim, A.S., Kosaka, M., Lee, C.Y., Watt, A., Grossman, T.R., Rosenfeld, M.G., Evans, R.M., Glass, C.K., 2013. Rev-Erbs repress macrophage gene expression by inhibiting enhancer-directed transcription. Nature 498, 511-515.

Lee, J., Ko, H.G., Kim, K., Kaang, B.K., 2016. Mildly Increased Mechanical Nociceptive Sensitivity in REV-ERBα Knock-out Mice. Exp Neurobiol 25, 342-346.

Li, Y., Zhang, H., Kosturakis, A.K., Jawad, A.B., Dougherty, P.M., 2014. Toll-like receptor 4 signaling contributes to Paclitaxel-induced peripheral neuropathy. J Pain 15, 712-725.

Loram, L.C., Taylor, F.R., Strand, K.A., Frank, M.G., Sholar, P., Harrison, J.A., Maier, S.F., Watkins, L.R., 2011. Prior exposure to glucocorticoids potentiates lipopolysaccharide induced mechanical allodynia and spinal neuroinflammation. Brain Behav Immun 25, 1408-1415.

Lu, Y., Cao, D.L., Jiang, B.C., Yang, T., Gao, Y.J., 2015. MicroRNA-146a-5p attenuates neuropathic pain via suppressing TRAF6 signaling in the spinal cord. Brain Behav Immun 49, 119-129.

Mika, J., Zychowska, M., Popiolek-Barczyk, K., Rojewska, E., Przewlocka, B., 2013. Importance of glial activation in neuropathic pain. Eur J Pharmacol 716, 106-119.

Morioka, N., Abe, H., Araki, R., Matsumoto, N., Zhang, F.F., Nakamura, Y., Hisaoka-Nakashima, K., Nakata, Y., 2014. A β1/2 adrenergic receptor-sensitive intracellular signaling pathway modulates CCL2 production in cultured spinal astrocytes. J Cell Physiol 229, 323-332.

Morioka, N., Fujii, S., Kondo, S., Zhang, F.F., Miyauchi, K., Nakamura, Y., Hisaoka-Nakashima, K., Nakata, Y., 2018. Downregulation of spinal astrocytic connexin43 leads to upregulation of interleukin-6 and cyclooxygenase-2 and mechanical hypersensitivity in mice. Glia 66, 428-444.

Morioka, N., Saeki, M., Sugimoto, T., Higuchi, T., Zhang, F.F., Nakamura, Y., Hisaoka-Nakashima, K., Nakata, Y., 2016a. Downregulation of the spinal dorsal horn clock gene Per1 expression leads to mechanical hypersensitivity via c-jun N-terminal kinase and CCL2 production in mice. Mol Cell Neurosci 72, 72-83.

Morioka, N., Tomori, M., Zhang, F.F., Saeki, M., Hisaoka-Nakashima, K., Nakata, Y., 2016b. Stimulation of nuclear receptor REV-ERBs regulates tumor necrosis factor-

induced expression of proinflammatory molecules in C6 astroglial cells. Biochem Biophys Res Commun 469, 151-157.

Morioka, N., Zhang, F.F., Nakamura, Y., Kitamura, T., Hisaoka-Nakashima, K., Nakata, Y., 2015. Tumor necrosis factor-mediated downregulation of spinal astrocytic connexin43 leads to increased glutamatergic neurotransmission and neuropathic pain in mice. Brain Behav Immun 49, 293-310.

Nakagawa, T., Kaneko, S., 2010. Spinal astrocytes as therapeutic targets for pathological pain. J Pharmacol Sci 114, 347-353.

Nakamura, Y., Morioka, N., Zhang, F.F., Hisaoka-Nakashima, K., Nakata, Y., 2015. Downregulation of connexin36 in mouse spinal dorsal horn neurons leads to mechanical allodynia. J Neurosci Res 93, 584-591.

Nakazato, R., Hotta, S., Yamada, D., Kou, M., Nakamura, S., Takahata, Y., Tei, H., Numano, R., Hida, A., Shimba, S., Mieda, M., Hinoi, E., Yoneda, Y., Takarada, T., 2017. The intrinsic microglial clock system regulates interleukin-6 expression. Glia 65, 198-208.

Pariollaud, M., Gibbs, J.E., Hopwood, T.W., Brown, S., Begley, N., Vonslow, R., Poolman, T., Guo, B., Saer, B., Jones, D.H., Tellam, J.P., Bresciani, S., Tomkinson, N.C., Wojno-Picon, J., Cooper, A.W., Daniels, D.A., Trump, R.P., Grant, D., Zuercher, W., Willson, T.M., MacDonald, A.S., Bolognese, B., Podolin, P.L., Sanchez, Y., Loudon, A.S., Ray, D.W., 2018. Circadian clock component REV-ERBα controls homeostatic regulation of pulmonary inflammation. J Clin Invest 128, 2281-2296.

Qian, B., Li, F., Zhao, L.X., Dong, Y.L., Gao, Y.J., Zhang, Z.J., 2016. Ligustilide Ameliorates Inflammatory Pain and Inhibits TLR4 Upregulation in Spinal Astrocytes Following Complete Freund's Adjuvant Peripheral Injection. Cell Mol Neurobiol 36, 143-149.

Ramakrishnan, S.N., Lau, P., Burke, L.J., Muscat, G.E., 2005. Rev-erbbeta regulates

the expression of genes involved in lipid absorption in skeletal muscle cells: evidence for cross-talk between orphan nuclear receptors and myokines. J Biol Chem 280, 8651-8659.

Saito, O., Svensson, C.I., Buczynski, M.W., Wegner, K., Hua, X.Y., Codeluppi, S., Schaloske, R.H., Deems, R.A., Dennis, E.A., Yaksh, T.L., 2010. Spinal glial TLR4-mediated nociception and production of prostaglandin E(2) and TNF. Br J Pharmacol 160, 1754-1764.

Sato, S., Sakurai, T., Ogasawara, J., Takahashi, M., Izawa, T., Imaizumi, K., Taniguchi, N., Ohno, H., Kizaki, T., 2014. A circadian clock gene, Rev-erbα, modulates the inflammatory function of macrophages through the negative regulation of Ccl2 expression. J Immunol 192, 407-417.

Shibata, K., Sugawara, T., Fujishita, K., Shinozaki, Y., Matsukawa, T., Suzuki, T., Koizumi, S., 2011. The astrocyte-targeted therapy by Bushi for the neuropathic pain in mice. PLoS One 6, e23510.

Sitaula, S., Billon, C., Kamenecka, T.M., Solt, L.A., Burris, T.P., 2015. Suppression of atherosclerosis by synthetic REV-ERB agonist. Biochem Biophys Res Commun 460, 566-571.

Solt, L.A., Wang, Y., Banerjee, S., Hughes, T., Kojetin, D.J., Lundasen, T., Shin, Y., Liu, J., Cameron, M.D., Noel, R., Yoo, S.H., Takahashi, J.S., Butler, A.A., Kamenecka, T.M., Burris, T.P., 2012. Regulation of circadian behaviour and metabolism by synthetic REV-ERB agonists. Nature 485, 62-68.

Song, C., Tan, P., Zhang, Z., Wu, W., Dong, Y., Zhao, L., Liu, H., Guan, H., Li, F., 2018. REV-ERB agonism suppresses osteoclastogenesis and prevents ovariectomy-induced bone loss partially via FABP4 upregulation. FASEB J 32, 3215-3228.

Stujanna, E.N., Murakoshi, N., Tajiri, K., Xu, D., Kimura, T., Qin, R., Feng, D., Yonebayashi, S., Ogura, Y., Yamagami, F., Sato, A., Nogami, A., Aonuma, K., 2017.

Rev-erb agonist improves adverse cardiac remodeling and survival in myocardial infarction through an anti-inflammatory mechanism. PLoS One 12, e0189330.

Sulli, G., Rommel, A., Wang, X., Kolar, M.J., Puca, F., Saghatelian, A., Plikus, M.V., Verma, I.M., Panda, S., 2018. Pharmacological activation of REV-ERBs is lethal in cancer and oncogene-induced senescence. Nature 553, 351-355.

Yin, L., Lazar, M.A., 2005. The orphan nuclear receptor Rev-erbalpha recruits the N-CoR/histone deacetylase 3 corepressor to regulate the circadian Bmal1 gene. Mol Endocrinol 19, 1452-1459.

Zhang, F.F., Morioka, N., Harano, S., Nakamura, Y., Liu, K., Nishibori, M., Hisaoka-Nakashima, K., Nakata, Y., 2016. Perineural expression of high-mobility group box-1 contributes to long-lasting mechanical hypersensitivity via matrix metalloprotease-9 up-regulation in mice with painful peripheral neuropathy. J Neurochem 136, 837-850.

Zhang, H., Yoon, S.Y., Dougherty, P.M., 2012a. Evidence that spinal astrocytes but not microglia contribute to the pathogenesis of Paclitaxel-induced painful neuropathy. J Pain 13, 293-303.

Zhang, X., Xu, Y., Wang, J., Zhou, Q., Pu, S., Jiang, W., Du, D., 2012b. The effect of intrathecal administration of glial activation inhibitors on dorsal horn BDNF overexpression and hind paw mechanical allodynia in spinal nerve ligated rats. J Neural Transm 119, 329-336.

Zhang, Y., Fang, B., Emmett, M.J., Damle, M., Sun, Z., Feng, D., Armour, S.M., Remsberg, J.R., Jager, J., Soccio, R.E., Steger, D.J., Lazar, M.A., 2015. GENE REGULATION. Discrete functions of nuclear receptor Rev-erbα couple metabolism to the clock. Science 348, 1488-1492.

Zhao, L.X., Jiang, B.C., Wu, X.B., Cao, D.L., Gao, Y.J., 2014. Ligustilide attenuates inflammatory pain via inhibition of NFκB-mediated chemokines production in spinal astrocytes. Eur J Neurosci 39, 1391-1402.

Zhu, M.D., Zhao, L.X., Wang, X.T., Gao, Y.J., Zhang, Z.J., 2014. Ligustilide inhibits microglia-mediated proinflammatory cytokines production and inflammatory pain. Brain Res Bull 109, 54-60.

Zhuang, Z.Y., Gerner, P., Woolf, C.J., Ji, R.R., 2005. ERK is sequentially activated in neurons, microglia, and astrocytes by spinal nerve ligation and contributes to mechanical allodynia in this neuropathic pain model. Pain 114, 149-159.

Figure Legends

Figure 1. Suppressive effect of SR9009 on LPS-induced upregulation of IL-1β mRNA (a), IL-6 mRNA (b), MMP-9 mRNA (c) and CCL2 mRNA (d) expression over time in cultured spinal astrocytes. After treatment with REV-ERB agonist SR9009 (10 μM) for 30 min, cells were then stimulated with LPS (10 ng/ml) for time periods indicated (1, 3, 6 and 24 hours). Then, expression levels of each mRNA were determined. Data are expressed as ratio of vehicle at each corresponding time point, and represent the mean± SEM for five independent experiments. *P<0.05, **P<0.01 vs. vehicle treatment. †P<0.05, ††P<0.01 vs. LPS treatment alone.

Figure 2. Effect of SR9009 on LPS-induced upregulation of IL-1β mRNA (a), IL-6 mRNA (b), MMP-9 mRNA (c) and CCL2 mRNA (d) expression in cultured spinal astrocytes. After treatment with REV-ERB agonist SR9009 (3, 5 or 10 μM) for 30 min, cells were then stimulated with LPS (10 ng/ml) for 24 hours. Cells were also treated with SR9009 in the absence of LPS. Data represent the mean±SEM for six to nine independent experiments. **P<0.01 vs. vehicle treatment. ††P<0.01 vs. LPS treatment alone.

Figure 3. Effect of GSK4112 on LPS-induced upregulation of IL-1β mRNA (a), IL-6

mRNA (b), MMP-9 mRNA (c) and CCL2 mRNA (d) expression in cultured spinal astrocytes. After treatment with REV-ERB agonist GSK4112 (10 or 20 μM) for 30 min, cells were then stimulated with LPS (10 ng/ml) for 24 hours. Cells were also treated with GSK4112 in the absence of LPS. Data represent the mean ± SEM for five independent experiments. **P<0.01 vs. vehicle treatment. †P<0.05, ††P<0.01 vs. LPS treatment alone.

Figure 4. Effect of SR9009 on TNF-induced upregulation of IL-1β mRNA (a), IL-6 mRNA (b), MMP-9 mRNA (c) and CCL2 mRNA (d) expression in cultured spinal astrocytes. After treatment with SR9009 (3 or 5 μM) for 30 min, cells were then stimulated with TNF (10 ng/ml) for 24 hours. Cells were also treated with SR9009 in the absence of TNF. Data represent the mean ± SEM for five independent experiments. **P<0.01 vs. vehicle treatment. †P<0.05, ††P<0.01 vs. LPS treatment alone.

Figure 5. Effects of SR9009 on LPS-induced upregulation of proinflammatory molecule protein expression in cultured spinal astrocytes. Effects of SR9009 on LPS-induced expression of IL-1β (a), IL-6 (b) and CCL2 (c) protein in cultured spinal astrocytes. After treatment with SR9009 (10 μM) for 30 min, cells were then

stimulated with LPS (10 ng/ml) for 24 hours. The expression levels of these proteins were measured by ELISA. Data represent the mean ± SEM for four independent experiments. *P<0.05, **P<0.01 vs. vehicle treatment. †P<0.05, ††P<0.01 vs. LPS treatment alone. (d) Effects of SR9009 on LPS-induced MMP-9 activity in cultured spinal astrocytes. After treatment with SR9009 (10 μM) for 30 min, cells were then stimulated with LPS (10 ng/ml) for 24 hours. The activity of MMP-9 was measured by zymography. The upper photograph is a representative zymography of MMP-9. Quantitative graph are shown below. Data represent the mean ± SEM for six independent experiments. **P<0.01 vs. vehicle treatment. †P<0.05 vs. LPS treatment alone.

Figure 6. REV-ERB activation is involved in the suppressed expression of proinflammatory molecules in cultured spinal astrocytes. (a) Silencing of Rev-erbα and Rev-erbβ expression in cultured spinal astrocytes. Cells were transfected with either non-targeting siRNA or a combination of Rev-erbα- and Rev-erbβ-tageting silencing interfering RNA (Rev-erbα/β siRNA). After 24 hours, Rev-erb mRNA expression levels were examined. Data represent the mean ± SEM for five independent experiments. **P<0.01 vs. non-targeting siRNA treatment. Downregulation of Rev-erbs expression by siRNA prevented the inhibitory effect of

SR9009 on LPS-induced upregulation of IL-1β mRNA (b), IL-6 mRNA (c) and MMP-9 mRNA (d) expression in cultured spinal astrocytes. After transfection with either non-targeting siRNA or a combination of Rev-erbα- and Rev-erbβ-targeting siRNA for 24 hours, astrocytes were treated with 5 μM of SR9009 for 30 min. Cells were then treated with 10 ng/ml of LPS for 24 hours. Data represent the mean±SEM for five independent experiments. **P<0.01 vs. LPS alone at each siRNA treatment. †P<0.05, ††P<0.01 vs. LPS + SR9009 at non-targeting siRNA.

Figure 7. HDAC3 is involved in REV-ERB-mediated inhibition of IL-1β mRNA and IL-6 mRNA expression, but not MMP-9 mRNA expression. After treatment with the selective HDAC3 inhibitor RGFP966 (2 μM) for 30 min, cells were incubated with SR9009 (5 μM) for 30 min and then LPS (10 ng/ml) for 24 hours. Cells were also incubated in RGFP966 (2 μM) in the absence of SR9009 and LPS. Expression levels of L-1β mRNA (a), IL-6 mRNA (b) and MMP-9 mRNA (c) relative to LPS-treated astrocytes are shown. Data represent the mean±SEM for five to eight independent experiments. **P<0.01 vs. vehicle treatment. †P<0.05, ††P<0.01 vs. LPS treatment alone. ##P<0.01 vs. SR9009+LPS treatment.

Figure 8. REV-ERBs agonists prevent mechanical hypersensitivity of mice intrathecally injected with LPS. One hour after intrathecal treatment with either SR9009 (100 or 300 nmol), GSK4112 (100 nmol) or DMSO, either LPS (0.1 μg) or saline was intrathecally injected and hind paw withdrawal thresholds were assessed over time. n=10-13/group. Data represent the mean ± SEM. *P<0.05, **P<0.01 vs. saline-injected mice with DMSO at the corresponding time point. †P<0.05, ††P<0.01 vs. LPS-injected mice with DMSO at the corresponding time point.

Figure 9. Activation of REV-ERBs reduces expression of IL-1β mRNA and IL-6 mRNA in spinal dorsal horn of mice intrathecally injected with LPS. Thirty minutes after intrathecal treatment with either SR9009 (100 or 300 nmol) or DMSO, either LPS (0.1 μg) or saline was intrathecally injected. Three hours later, spinal dorsal horn expression levels of L-1β mRNA (a), IL-6 mRNA (b) and MMP-9 mRNA (c) were measured. n=7-10/group. Data represent the mean ± SEM. **P<0.01 vs. saline-injected mice with DMSO. †P<0.05, ††P<0.01 vs. LPS-injected mice with DMSO.

Figure 10. Activation of REV-ERB prevents GFAP expression in spinal dorsal horn of mice intrathecally injected with LPS. (a) Thirty minutes after intrathecal treatment with either SR9009 (300 nmol) or DMSO, either LPS (0.1 μg) or saline was intrathecally

injected. Spinal dorsal horn was harvested 3 hours after LPS injection. Magnified photomicrographs of the white boxed areas are to the right. Scar bar=100 μm. (b) Quantitative analysis of expression of GFAP in spinal dorsal horn after injection of drugs described above at 3 hours following LPS injection. Data indicate mean ratio of sum of GFAP immunofluorescence intensity in each mice, and expressed as mean ± SEM for six to eight mice. **P<0.01 vs. saline-injected mice with DMSO. †P<0.05 vs. LPS-injected mice with DMSO.

Figure 11. Activation of REV-ERBs ameliorates mechanical hypersensitivity in mouse models of both inflammatory and neuropathic pain. a) Seven days after intraplantar treatment with either CFA or saline, either SR9009 (100 or 300 nmol) or DMSO was intrathecally injected and hind paw withdrawal thresholds were assessed over time. n=10/group. Data represent the mean ± SEM. **P<0.01 vs. saline-injected mice with DMSO at the corresponding time point. ††P<0.01 vs. CFA-injected mice with DMSO at the corresponding time point. b) Fourteen days after sciatic nerve injury, either SR9009 (100 or 300 nmol) or DMSO was intrathecally injected and hind paw withdrawal thresholds were assessed over time. n=11-14/group. Data represent the mean ± SEM. **P<0.01 vs. sham mice with vehicle at the corresponding time point. †P<0.05, ††P<0.01 vs. PSNL mice with vehicle at the corresponding time point. c)

Fourteen days after intraperitoneal treatment with either paclitaxel (PTX) or vehicle (6 days after last injection), either SR9009 (100 or 300 nmol) or DMSO was intrathecally injected and hind paw withdrawal thresholds were assessed over time. n=5-8/group. Data represent the mean ± SEM. *P<0.05, **P<0.01 vs. vehicle-injected mice with DMSO at the corresponding time point. †P<0.05, ††P<0.01 vs. PTX-injected mice with DMSO at the corresponding time point. d) Twenty one days after intraperitoneal treatment with either streptozotocin (STZ) or saline, either SR9009 (100 or 300 nmol) or DMSO was intrathecally injected and hind paw withdrawal thresholds were assessed over time. n=5-9/group. Data represent the mean ± SEM. **P<0.01 vs. vehicle-injected mice with DMSO at the corresponding time point. ††P<0.01 vs. PTX-injected mice with DMSO at the corresponding time point.

Figure 12. Activation of REV-ERB prevents GFAP expression in spinal dorsal horn of mice with PSNL. (a) Fourteen days after sciatic nerve injury, either SR9009 (300 nmol) or DMSO was intrathecally injected. Spinal dorsal horn was harvested 3 hours after SR9009 injection. Magnified photomicrographs of the white boxed areas are to the right. Scar bar=100 μm. (b) Quantitative analysis of expression of GFAP in spinal dorsal horn after injection of drugs described above at 3 hours following SR9009 injection. Data indicate mean ratio of sum of GFAP immunofluorescence intensity in

each mice, and expressed as mean ± SEM for six to eight mice. *P<0.05 vs. saline-injected mice with DMSO. †P<0.05 vs. LPS-injected mice with DMSO.

Figure 1

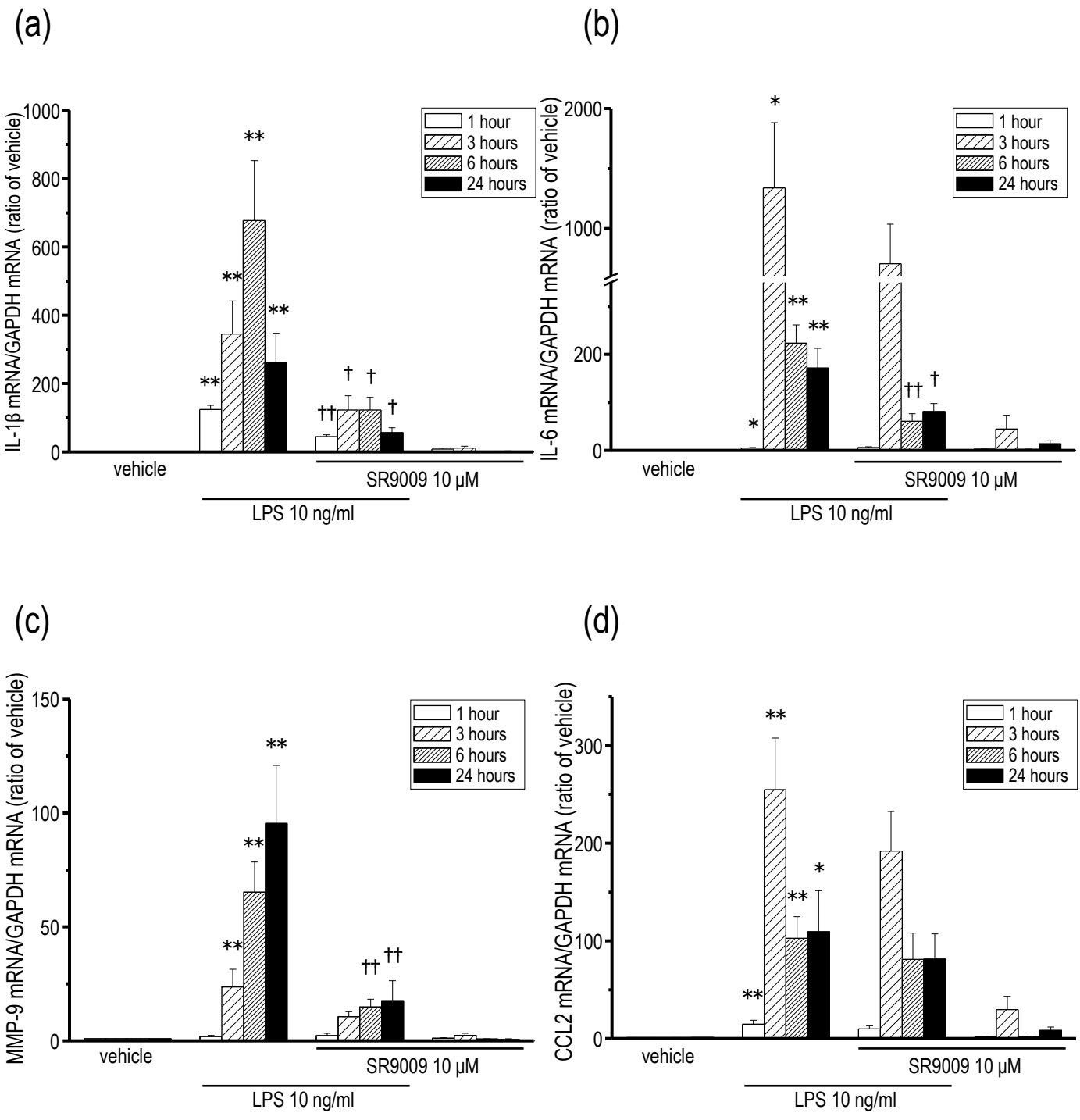
(a)
IL-1β mRNA/GAPDH mRNA (ratio of vehicle)
1000
800
600
400
200
0
1 hour
3 hours
6 hours
24 hours
**
**
**
**
††
†
†
†
vehicle
SR9009 10 μM
LPS 10 ng/ml
(b)
IL-6 mRNA/GAPDH mRNA (ratio of vehicle)
2000
1000
200
0
1 hour
3 hours
6 hours
24 hours
*
*
**
**
††
†
vehicle
SR9009 10 μM
LPS 10 ng/ml
(c)
MMP-9 mRNA/GAPDH mRNA (ratio of vehicle)
150
100
50
0
1 hour
3 hours
6 hours
24 hours
**
**
**
††
††
vehicle
SR9009 10 μM
LPS 10 ng/ml
(d)
CCL2 mRNA/GAPDH mRNA (ratio of vehicle)
300
200
100
0
1 hour
3 hours
6 hours
24 hours
**
**
**
*
vehicle
SR9009 10 μM
LPS 10 ng/ml

Figure 2

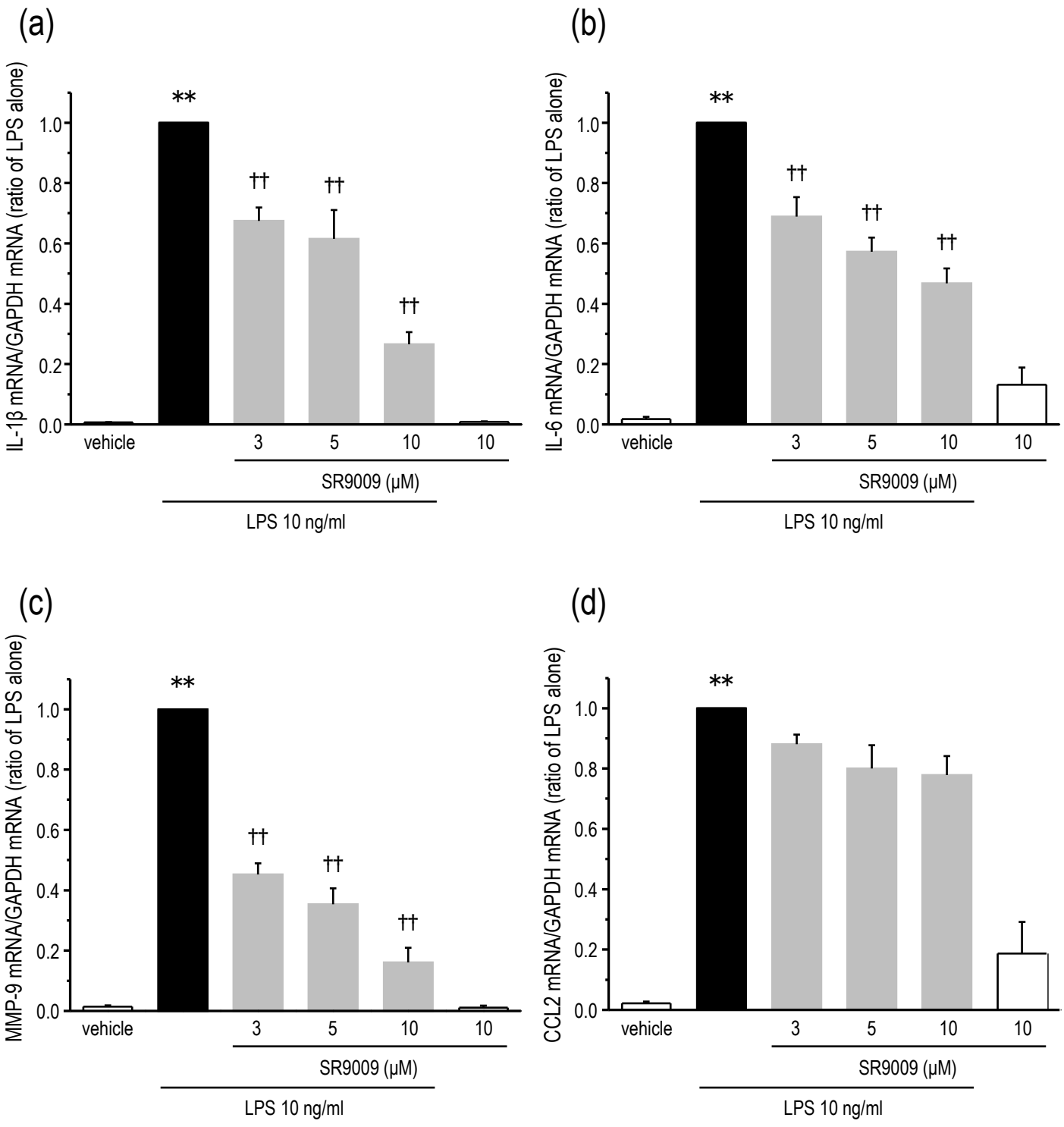
(a)
IL-1β mRNA/GAPDH mRNA (ratio of LPS alone)
1.0
0.8
0.6
0.4
0.2
0.0
**
††
††
††
vehicle
3
5
10
10
SR9009 (μM)
LPS 10 ng/ml
(b)
IL-6 mRNA/GAPDH mRNA (ratio of LPS alone)
**
††
††
††
vehicle
3
5
10
10
SR9009 (μM)
LPS 10 ng/ml
(c)
MMP-9 mRNA/GAPDH mRNA (ratio of LPS alone)
**
††
††
††
vehicle
3
5
10
10
SR9009 (μM)
LPS 10 ng/ml
(d)
CCL2 mRNA/GAPDH mRNA (ratio of LPS alone)
**
vehicle
3
5
10
10
SR9009 (μM)
LPS 10 ng/ml

Figure 3

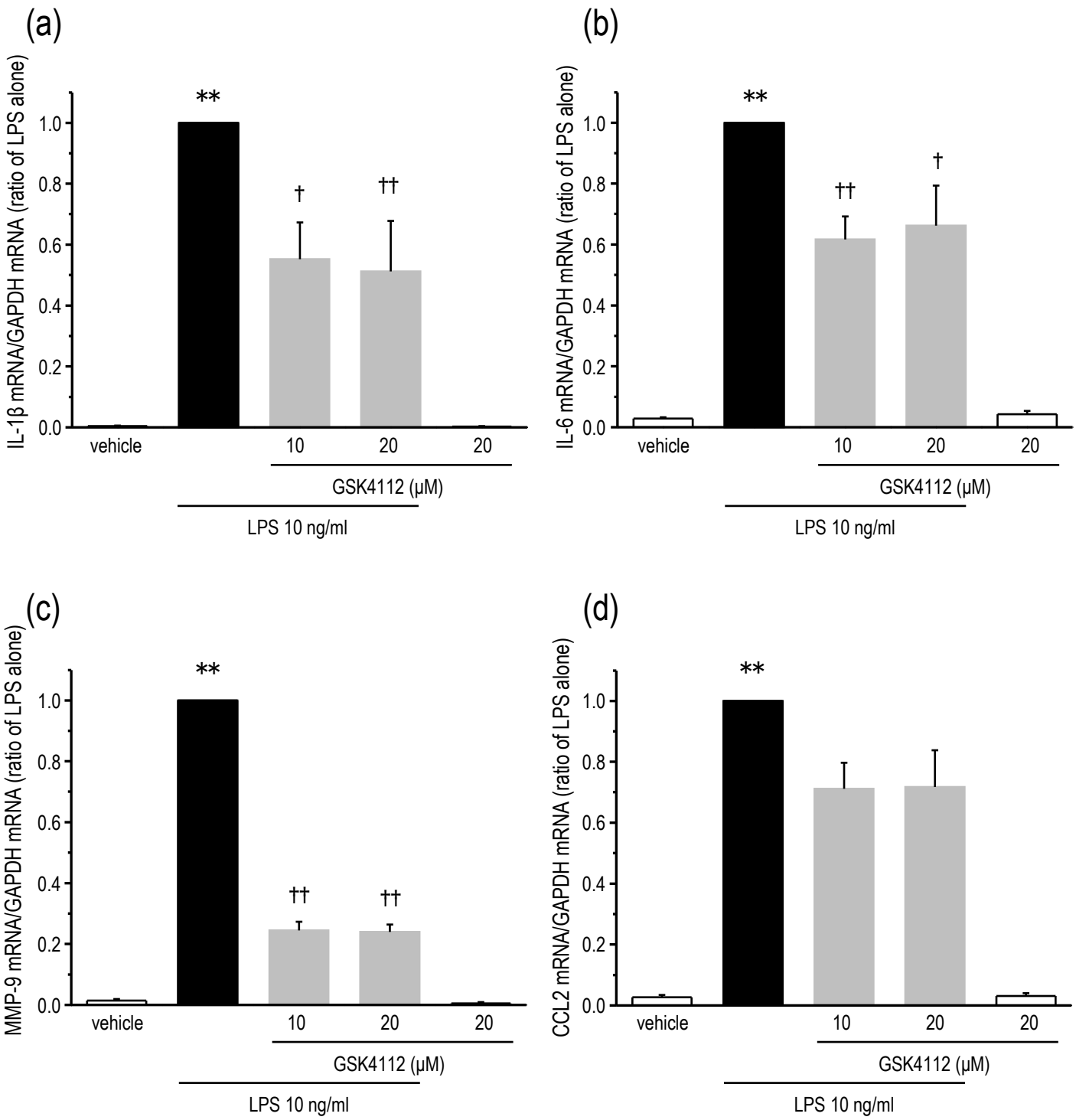
(a)
IL-1β mRNA/GAPDH mRNA (ratio of LPS alone)
1.0
0.8
0.6
0.4
0.2
0.0
**
†
††
vehicle
10
20
20
GSK4112 (μM)
LPS 10 ng/ml
(b)
IL-6 mRNA/GAPDH mRNA (ratio of LPS alone)
**
††
†
vehicle
10
20
20
GSK4112 (μM)
LPS 10 ng/ml
(c)
MMP-9 mRNA/GAPDH mRNA (ratio of LPS alone)
**
††
††
vehicle
10
20
20
GSK4112 (μM)
LPS 10 ng/ml
(d)
CCL2 mRNA/GAPDH mRNA (ratio of LPS alone)
**
vehicle
10
20
20
GSK4112 (μM)
LPS 10 ng/ml

Figure 4

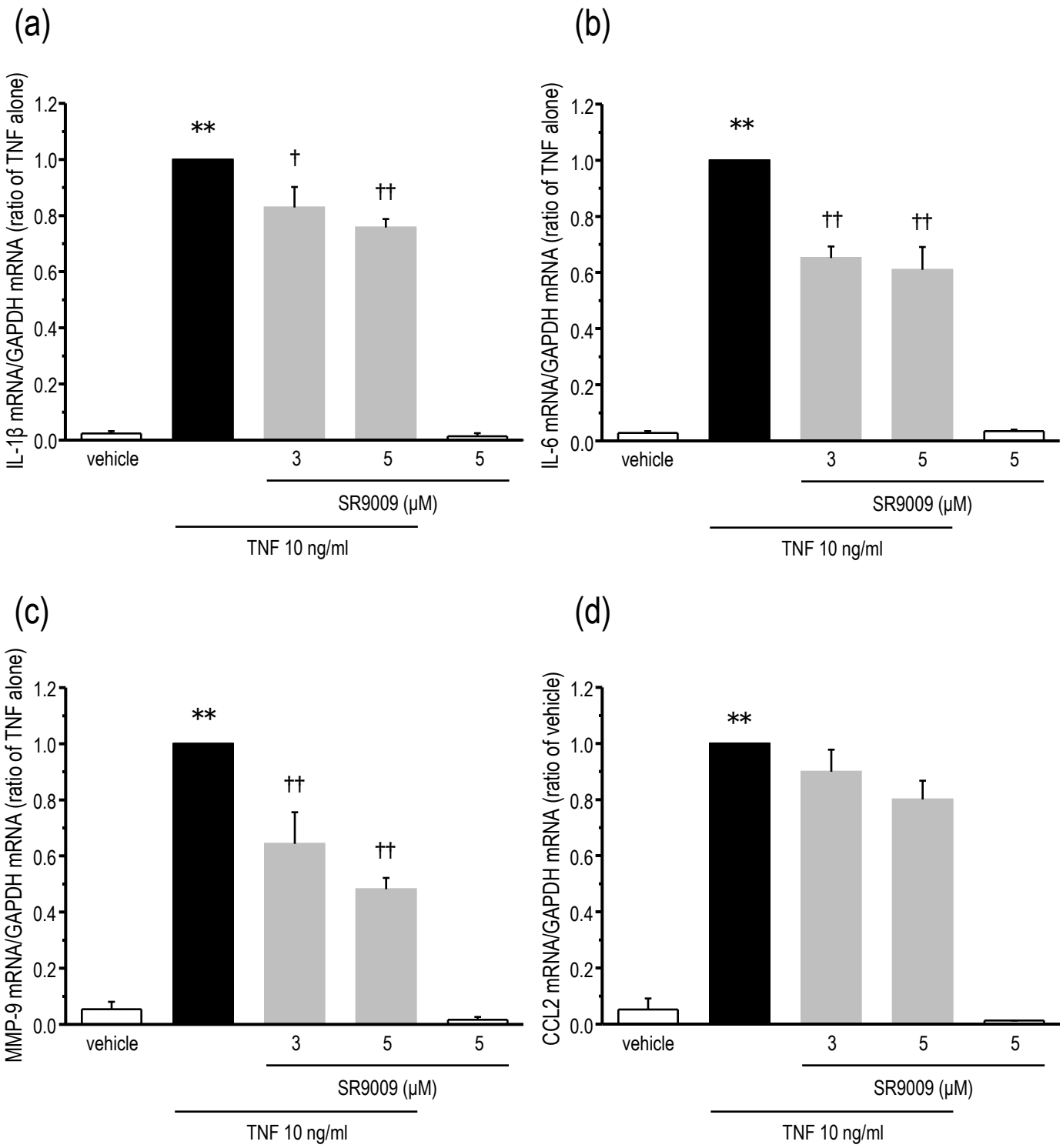
(a)
IL-1β mRNA/GAPDH mRNA (ratio of TNF alone)
1.2
1.0
0.8
0.6
0.4
0.2
0.0
**
†
††
vehicle
3
5
5
SR9009 (μM)
TNF 10 ng/ml
(b)
IL-6 mRNA/GAPDH mRNA (ratio of TNF alone)
**
††
††
vehicle
3
5
5
SR9009 (μM)
TNF 10 ng/ml
(c)
MMP-9 mRNA/GAPDH mRNA (ratio of TNF alone)
**
††
††
vehicle
3
5
5
SR9009 (μM)
TNF 10 ng/ml
(d)
CCL2 mRNA/GAPDH mRNA (ratio of vehicle)
**
vehicle
3
5
5
SR9009 (μM)
TNF 10 ng/ml

Figure 5

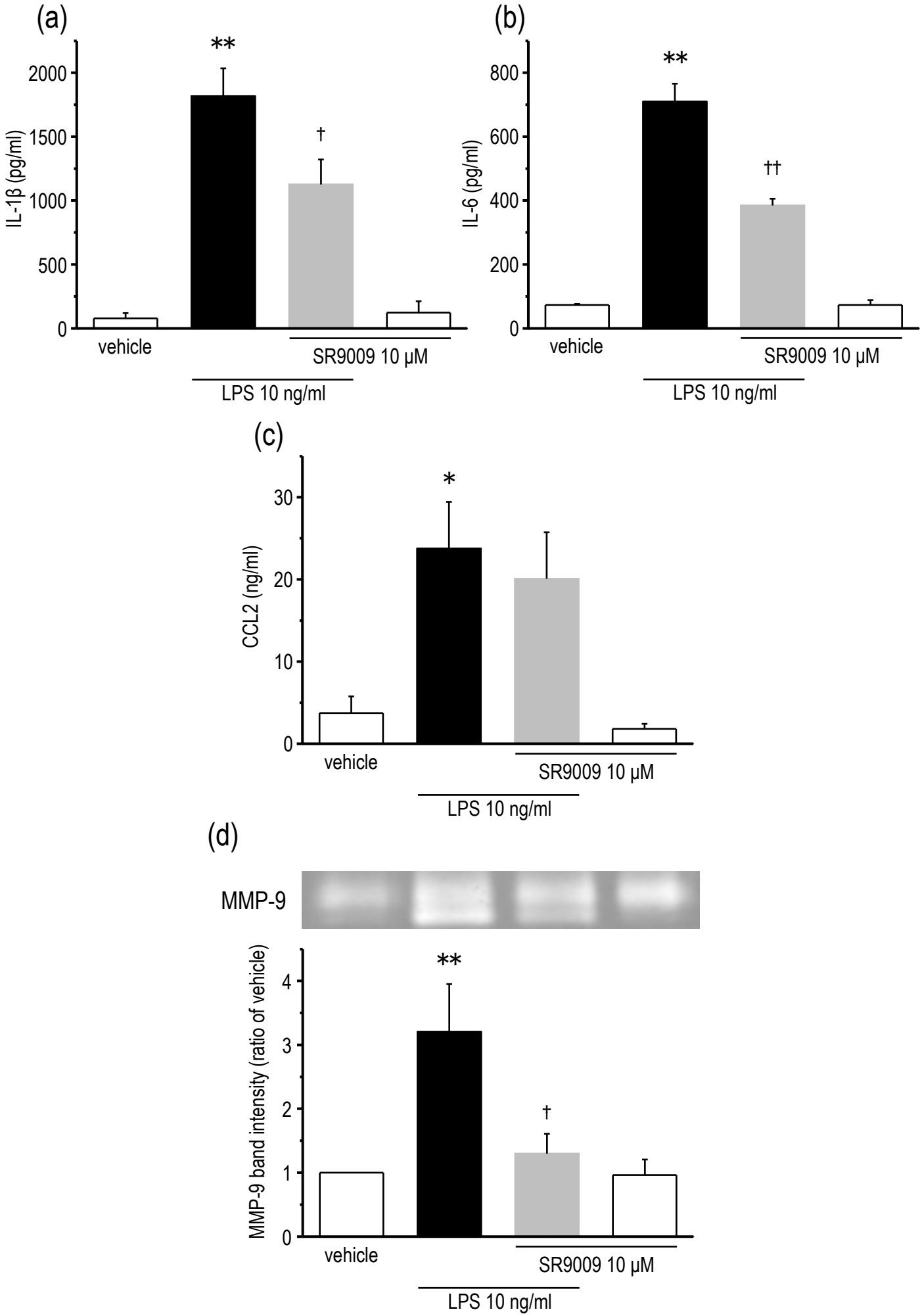
(a)
IL-1β (pg/ml)
2000
1500
1000
500
0
**
†
vehicle
SR9009 10 μM
LPS 10 ng/ml
(b)
IL-6 (pg/ml)
800
600
400
200
0
**
††
vehicle
SR9009 10 μM
LPS 10 ng/ml
(c)
CCL2 (ng/ml)
30
20
10
0
*
vehicle
SR9009 10 μM
LPS 10 ng/ml
(d)
MMP-9
MMP-9 band intensity (ratio of vehicle)
4
3
2
1
0
**
†
vehicle
SR9009 10 μM
LPS 10 ng/ml

Figure 6

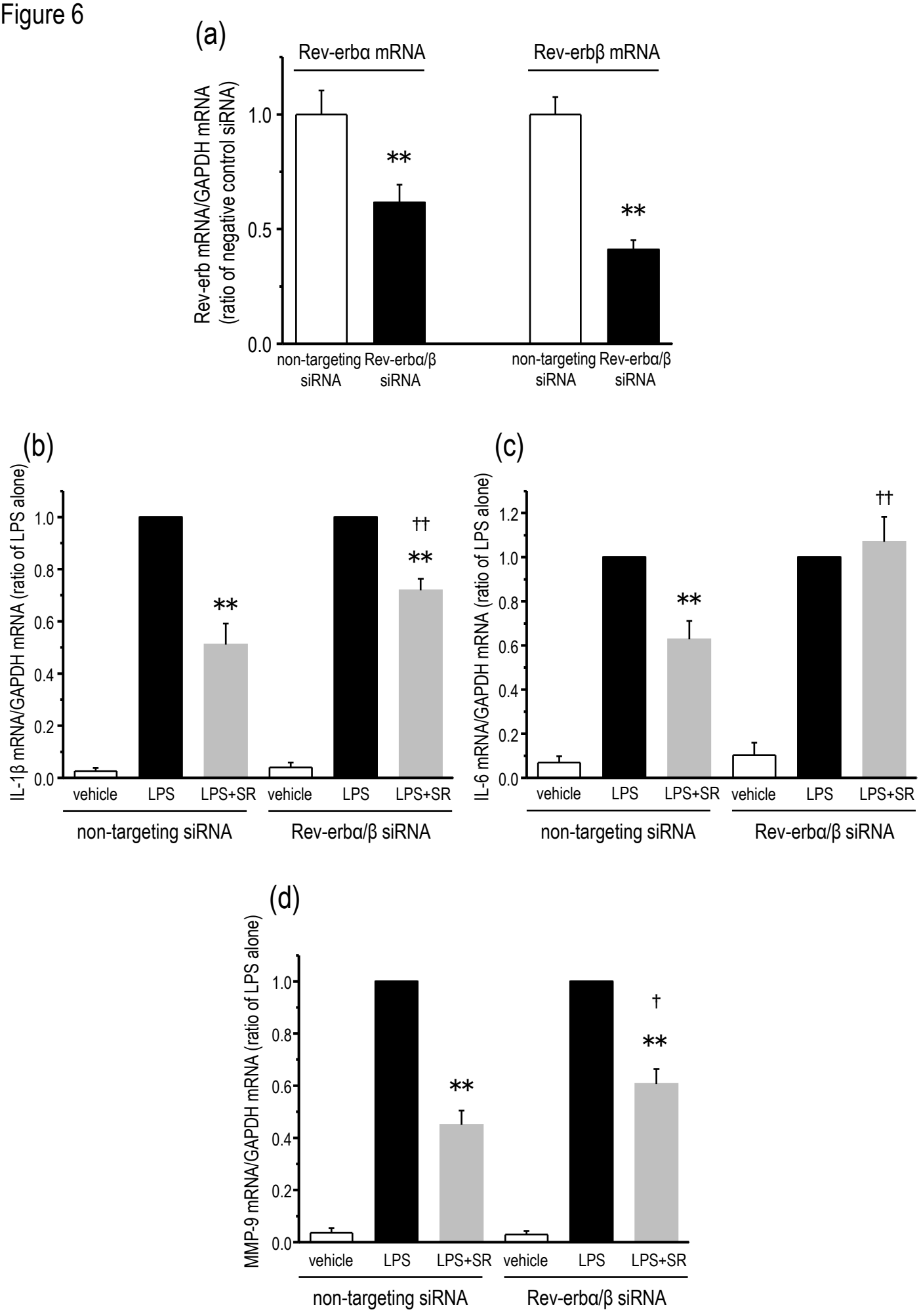
(a)
Rev-erbα mRNA
Rev-erbβ mRNA
Rev-erb mRNA/GAPDH mRNA
(ratio of negative control siRNA)
1.0
0.5
0.0
**
**
non-targeting siRNA
Rev-erbα/β siRNA
non-targeting siRNA
Rev-erbα/β siRNA
(b)
IL-1β mRNA/GAPDH mRNA (ratio of LPS alone)
1.0
0.8
0.6
0.4
0.2
0.0
**
††
**
vehicle
LPS
LPS+SR
vehicle
LPS
LPS+SR
non-targeting siRNA
Rev-erbα/β siRNA
(c)
IL-6 mRNA/GAPDH mRNA (ratio of LPS alone)
1.2
1.0
0.8
0.6
0.4
0.2
0.0
**
††
vehicle
LPS
LPS+SR
vehicle
LPS
LPS+SR
non-targeting siRNA
Rev-erbα/β siRNA
(d)
MMP-9 mRNA/GAPDH mRNA (ratio of LPS alone)
1.0
0.8
0.6
0.4
0.2
0.0
**
†
**
vehicle
LPS
LPS+SR
vehicle
LPS
LPS+SR
non-targeting siRNA
Rev-erbα/β siRNA

Figure 7

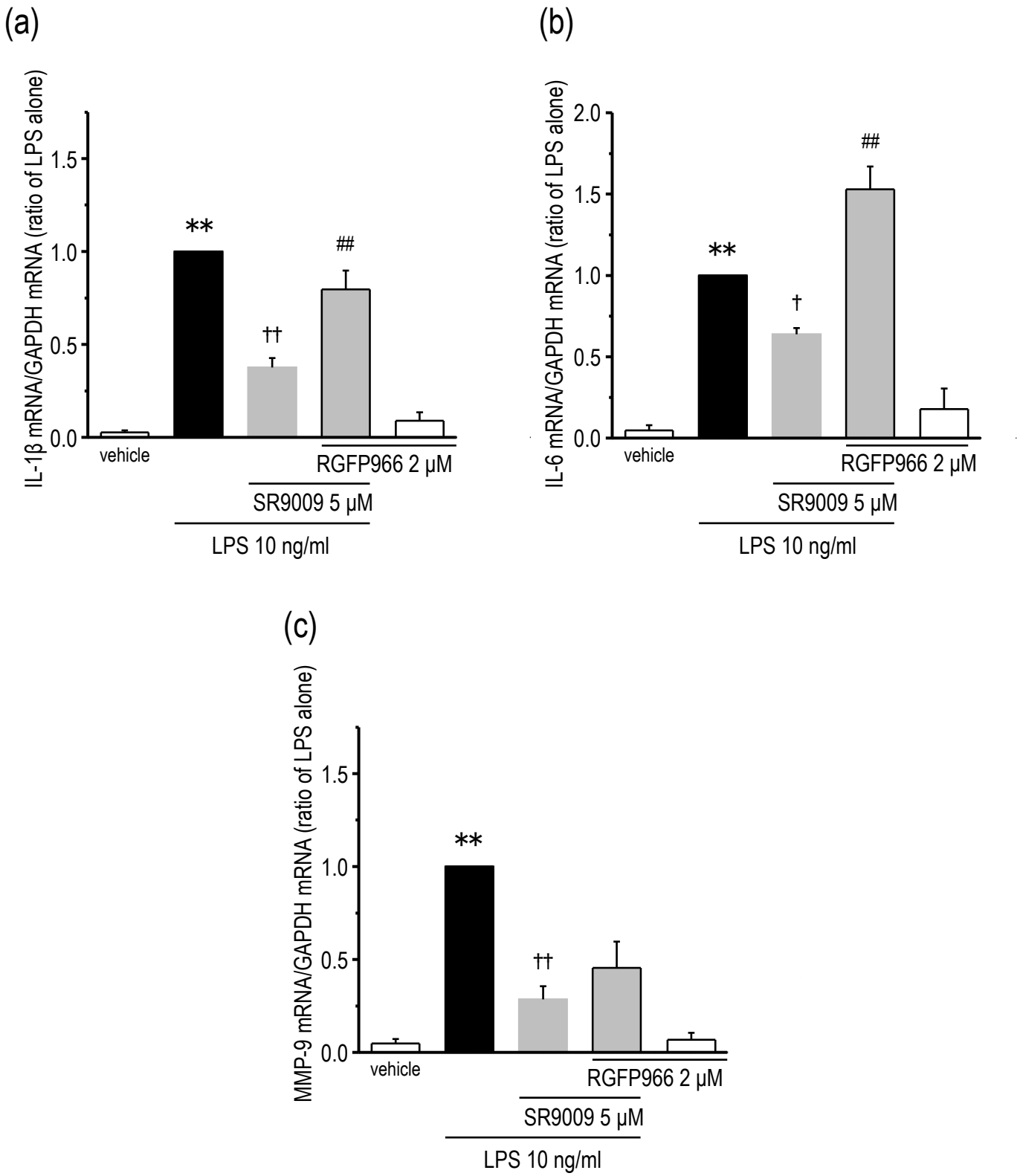
(a)
IL-1β mRNA/GAPDH mRNA (ratio of LPS alone)
0.0
0.5
1.0
1.5
**
††
##
vehicle
RGFP966 2 μM
SR9009 5 μM
LPS 10 ng/ml
(b)
IL-6 mRNA/GAPDH mRNA (ratio of LPS alone)
0.0
0.5
1.0
1.5
2.0
**
†
##
vehicle
RGFP966 2 μM
SR9009 5 μM
LPS 10 ng/ml
(c)
MMP-9 mRNA/GAPDH mRNA (ratio of LPS alone)
0.0
0.5
1.0
1.5
**
††
vehicle
RGFP966 2 μM
SR9009 5 μM
LPS 10 ng/ml

Figure 8

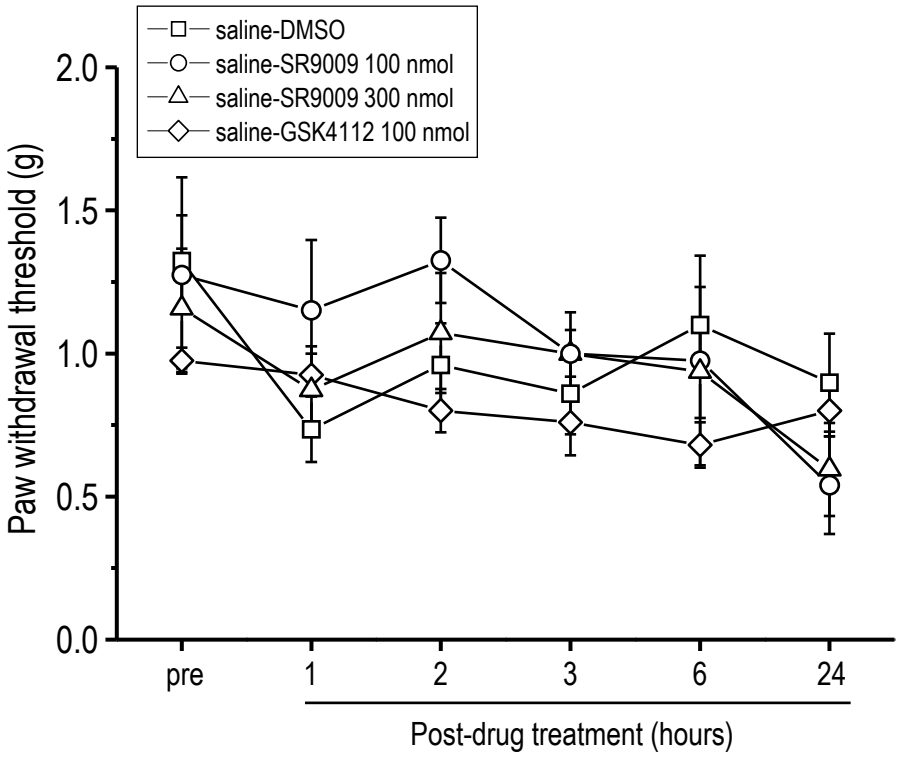
saline-DMSO
saline-SR9009 100 nmol
saline-SR9009 300 nmol
saline-GSK4112 100 nmol
Paw withdrawal threshold (g)
2.0
1.5
1.0
0.5
0.0
pre
1
2
3
6
24
Post-drug treatment (hours)

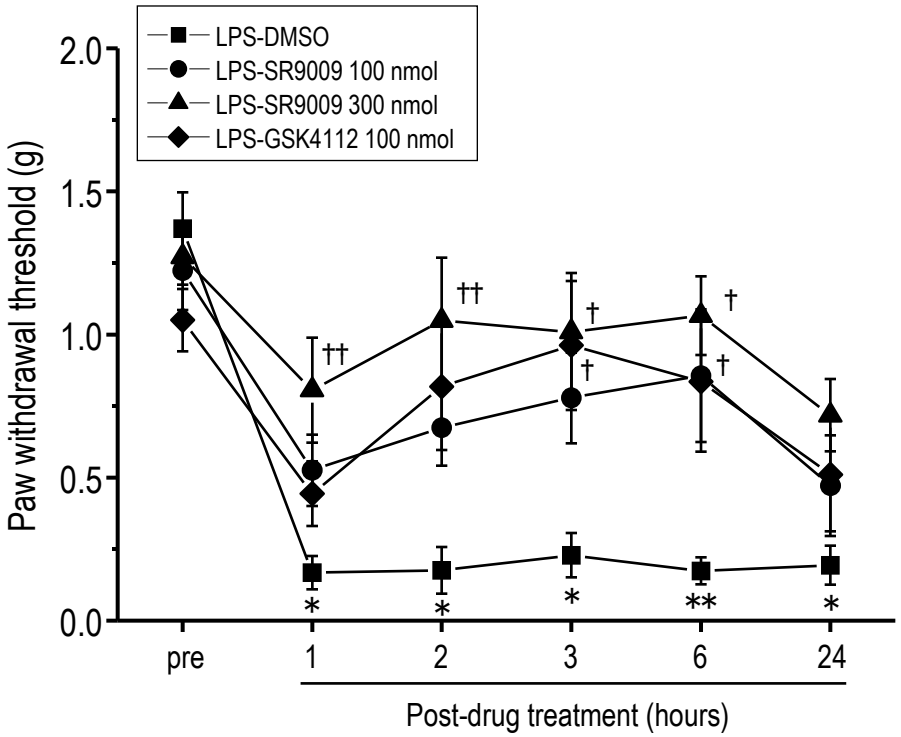
LPS-DMSO
LPS-SR9009 100 nmol
LPS-SR9009 300 nmol
LPS-GSK4112 100 nmol
Paw withdrawal threshold (g)
2.0
1.5
1.0
0.5
0.0
††
††
†
†
†
*
*
*
**
*
pre
1
2
3
6
24
Post-drug treatment (hours)

Figure 9

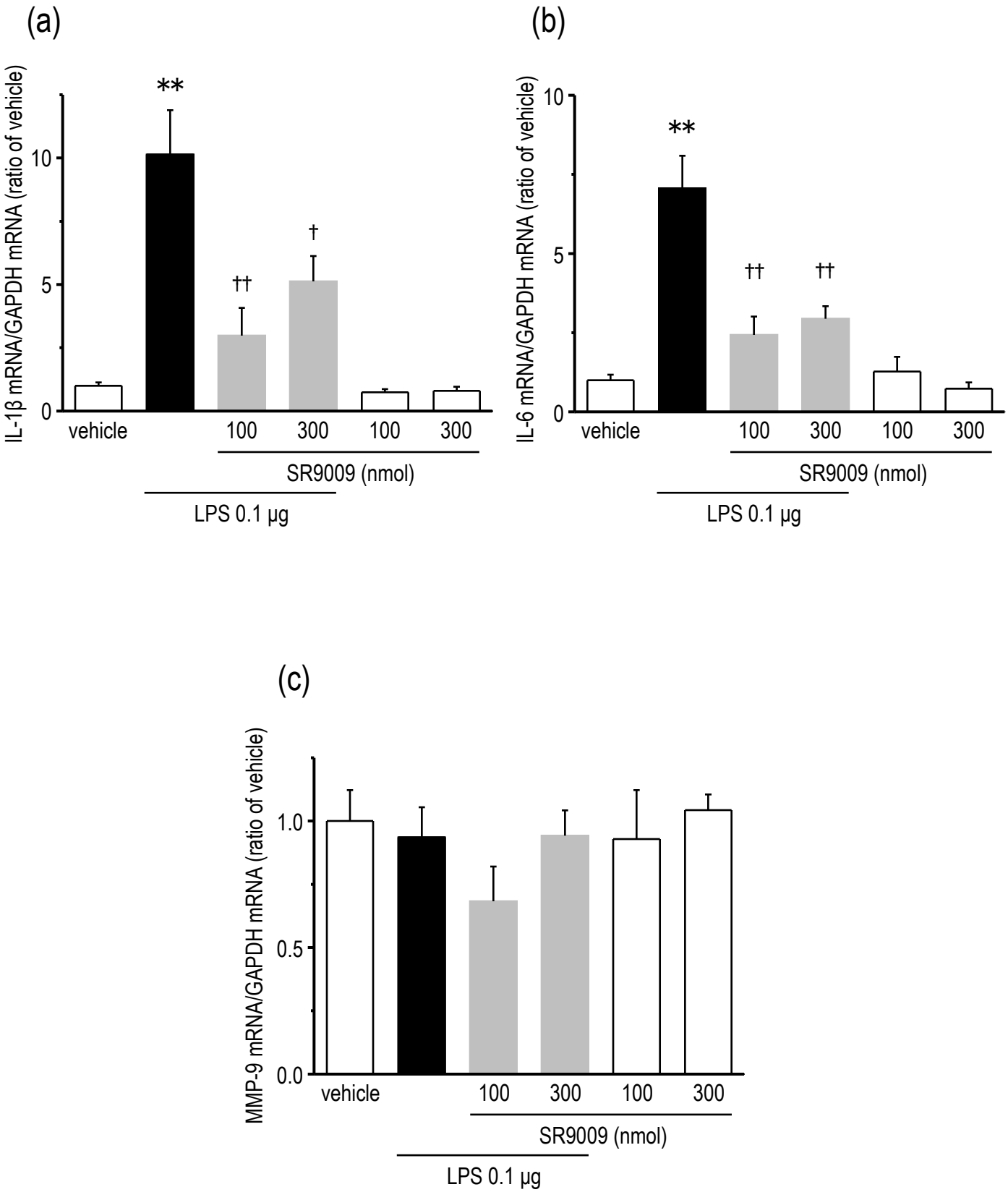
(a)
IL-1β mRNA/GAPDH mRNA (ratio of vehicle)
10
5
0
**
††
†
vehicle
100
300
100
300
SR9009 (nmol)
LPS 0.1 μg
(b)
IL-6 mRNA/GAPDH mRNA (ratio of vehicle)
10
5
0
**
††
††
vehicle
100
300
100
300
SR9009 (nmol)
LPS 0.1 μg
(c)
MMP-9 mRNA/GAPDH mRNA (ratio of vehicle)
1.0
0.5
0.0
vehicle
100
300
100
300
SR9009 (nmol)
LPS 0.1 μg

Figure 10

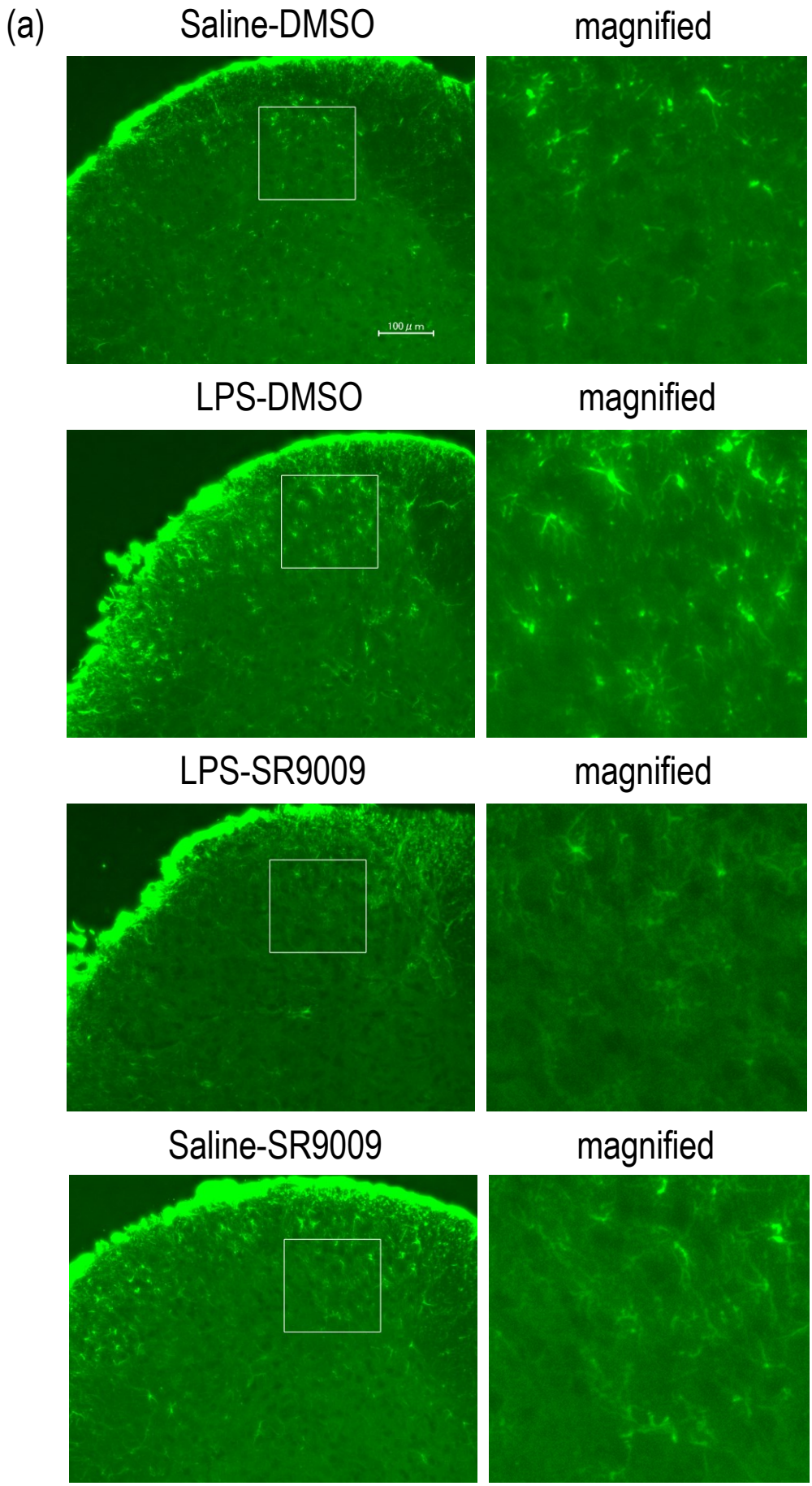
(a)
Saline-DMSO
magnified
100 μm
LPS-DMSO
magnified
LPS-SR9009
magnified
Saline-SR9009
magnified

Figure 10

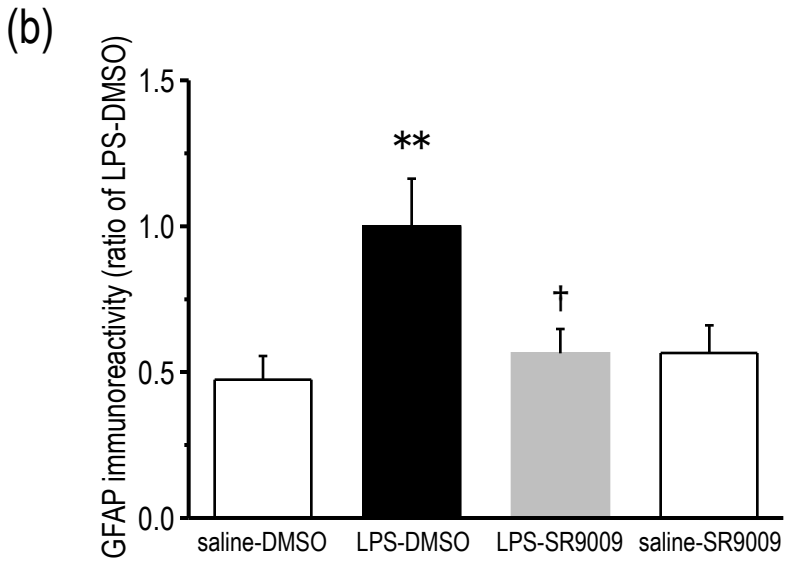
(b)
GFAP immunoreactivity (ratio of LPS-DMSO)
1.5
1.0
0.5
0.0
**
†
saline-DMSO
LPS-DMSO
LPS-SR9009
saline-SR9009

Figure 11

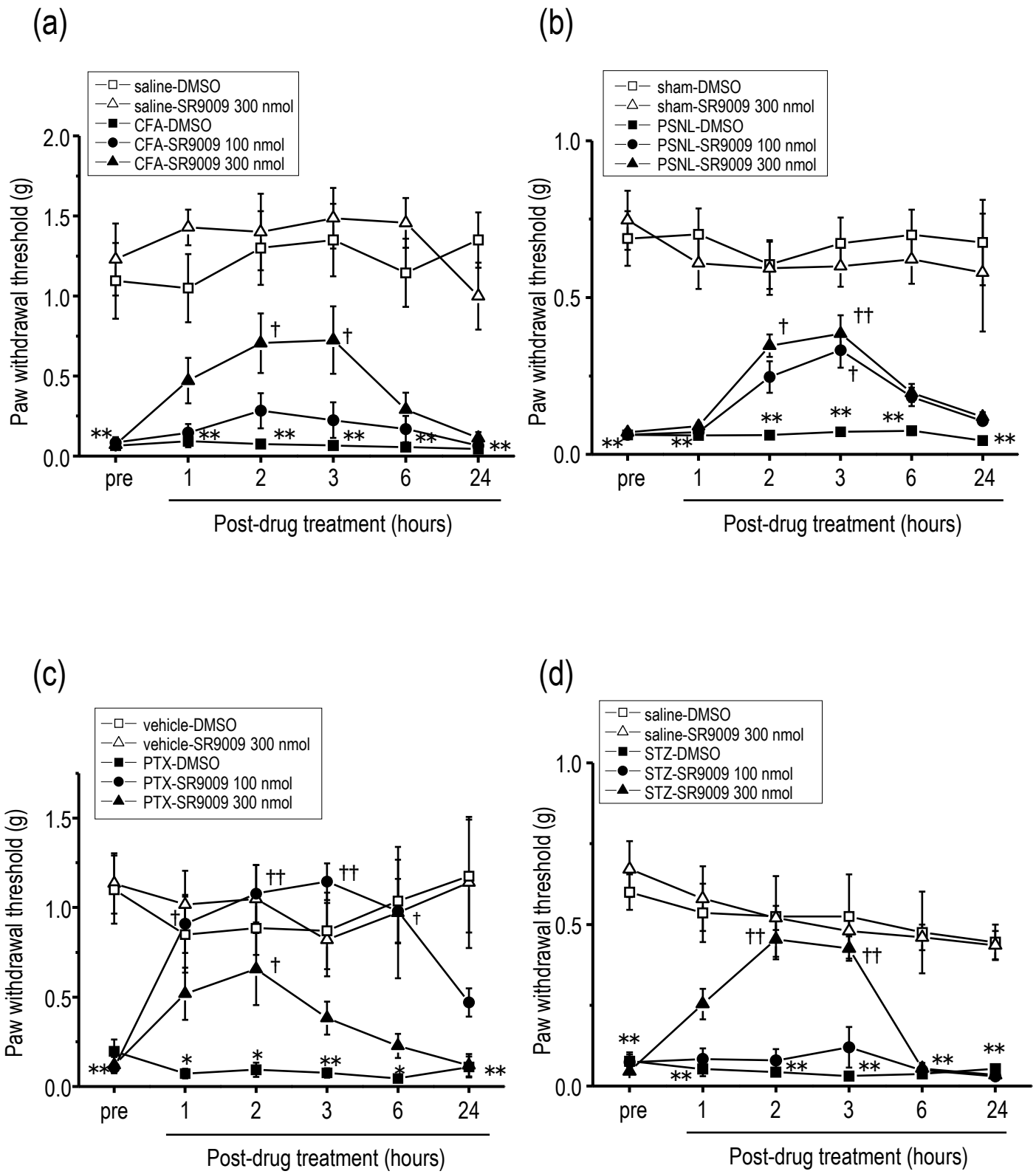
(a)
saline-DMSO
saline-SR9009 300 nmol
CFA-DMSO
CFA-SR9009 100 nmol
CFA-SR9009 300 nmol
Paw withdrawal threshold (g)
2.0
1.5
1.0
0.5
0.0
pre
1
2
3
6
24
Post-drug treatment (hours)
(b)
sham-DMSO
sham-SR9009 300 nmol
PSNL-DMSO
PSNL-SR9009 100 nmol
PSNL-SR9009 300 nmol
Paw withdrawal threshold (g)
1.0
0.5
0.0
pre
1
2
3
6
24
Post-drug treatment (hours)
(c)
vehicle-DMSO
vehicle-SR9009 300 nmol
PTX-DMSO
PTX-SR9009 100 nmol
PTX-SR9009 300 nmol
Paw withdrawal threshold (g)
1.5
1.0
0.5
0.0
pre
1
2
3
6
24
Post-drug treatment (hours)
(d)
saline-DMSO
saline-SR9009 300 nmol
STZ-DMSO
STZ-SR9009 100 nmol
STZ-SR9009 300 nmol
Paw withdrawal threshold (g)
1.0
0.5
0.0
pre
1
2
3
6
24
Post-drug treatment (hours)

Figure 12

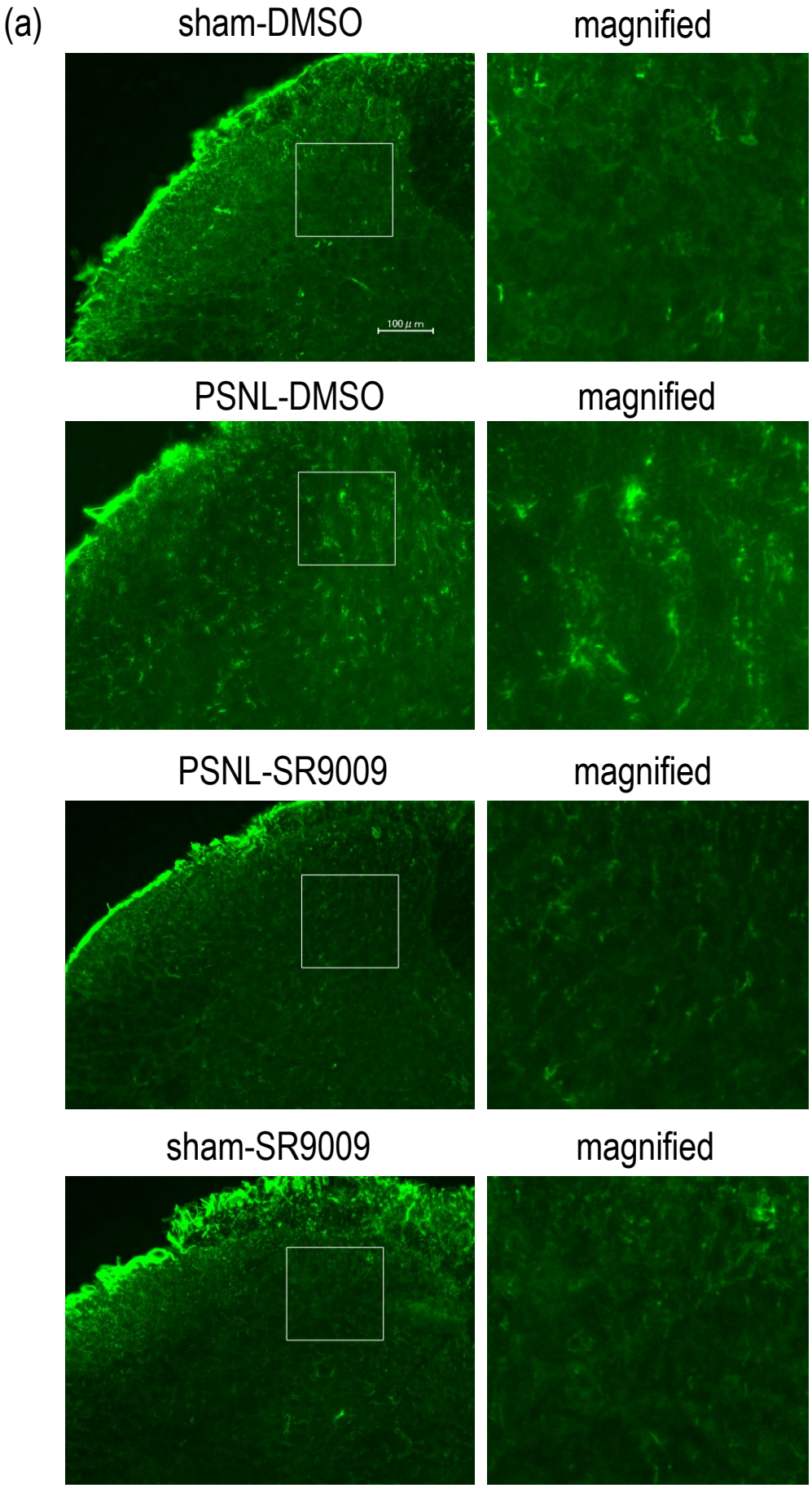
(a)
sham-DMSO
magnified
100 μm
PSNL-DMSO
magnified
PSNL-SR9009
magnified
sham-SR9009
magnified

Figure 12

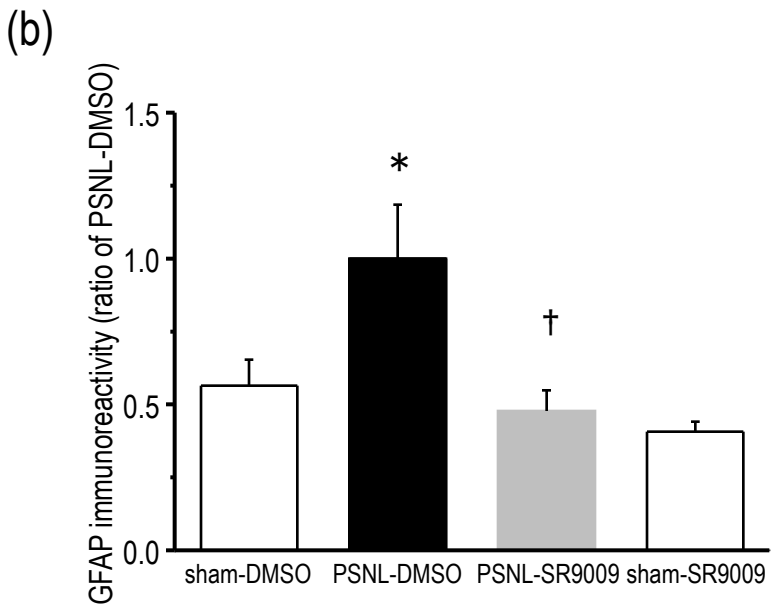
(b)
GFAP immunoreactivity (ratio of PSNL-DMSO)
1.5
1.0
0.5
0.0
*
†
sham-DMSO
PSNL-DMSO
PSNL-SR9009
sham-SR9009